NREL/TP-214-4606 • UC Category: 273 • DE92001176

NREL/TP--214-4606

DE92 001176

Manufacturing Technology Development for $CuInGaSe_2$ Solar Cell Modules

Final Subcontract Report 9 January 1991 — 14 April 1991

B.J. Stanbery
Boeing Aerospace & Electronics
Seattle, Washington

NREL technical monitor: R. Mitchell

National Renewable Energy Laboratory
(formerly the Solar Energy Research Institute)
1617 Cole Boulevard
Golden, Colorado 80401-3393
A Division of Midwest Research Institute
Operated for the U.S. Department of Energy
under Contract No. DE-AC02-83CH10093

Prepared under Subcontract No. XC-1-10057-14

November 1991

On September 16, 1991, the Solar Energy Research Institute was designated a national laboratory, and its name was changed to the National Renewable Energy Laboratory.

NOTICE

Printed in the United States of America
Available from:
National Technical Information Service
U.S. Department of Commerce
5285 Port Royal Road
Springfield, VA 22161

Price: Microfiche A01
Printed Copy A04

Codes are used for pricing all publications. The code is determined by the number of pages in the publication. Information pertaining to the pricing codes can be found in the current issue of the following publications which are generally available in most libraries: *Energy Research Abstracts (ERA)*; *Government Reports Announcements* and Index (*GRA* and I); *Scientific and Technical Abstract Reports (STAR)*; and publication NTIS-PR-360 available from NTIS at the above address.

Table of Contents

List of Figures

1. INTRODUCTION: CIGS MODULE MANUFACTURING TECHNOLOGY

Boeing Aerospace & Electronics is pleased to submit this Final Report to the Solar Energy Research Institute (SERI) in fulfillment of the Statement of Work reporting requirements for Subcontract No. XC-1-10057-14, "Photovoltaic Manufacturing Technology — Phase I." This Final Report addresses the identification and elimination of obstacles to the advancement of photovoltaic (PV) manufacturing technology in order to reduce module production costs, increase module performance, and increase PV production capacity in the United States.

Our subcontractors, Glasstech Solar, Inc. (GSI) and Advanced Technology Materials (ATM), have contributed to this study their unique capabilities which complement the technical expertise and terrestrial photovoltaic technology commercialization strategy of The Boeing Company. Their specific contributions to this plan for the advancement and development of PV manufacturing technology are incorporated herein.

Flat plate crystalline silicon modules dominate the photovoltaic power market, and thin–film modules have been identified in the DOE Five Year Plan as a leading contender to solve the cost problem of that technology. This is a consequence of the vastly smaller quantities of semiconductor material used, and the potential for low-cost, large–area production techniques. The Boeing Company has continued to play a key role in pioneering thin–film solar cell technology ever since our seminal demonstration of the first 10%-efficient polycrystalline $CuInSe_2$ (CIS) cell in 1980. The world's first monolithically integrated $CuInSe_2$ thin–film submodule was demonstrated by Boeing in 1984, subsequently achieving a 9.6% efficiency over a ~100 cm^2 area. Boeing developed a $CuIn_{1-x}Ga_xSe_2$ (CIGS) thin–film solar cell for SERI under its most recent subcontract, which achieved an efficiency of 12.5%, the highest ever measured by SERI for a polycrystalline or amorphous thin–film cell. Most recently Boeing, in collaboration with Kopin Corporation, has demonstrated a world thin–film solar cell efficiency record of 25.8% as measured by SERI, utilizing a thin–film tandem CLEFT GaAs/$CuInSe_2$ cell. This long-standing record of performance and leadership in the field of thin–film solar cells clearly establishes the technical expertise and abilities of the Boeing team to overcome problems that impede progress.

During the course of the research activities discussed above, Boeing has periodically evaluated the commercial potential of its technology in order to guide its business and investment strategy. The result has been (1) a substantial investment by Boeing in CIS technology, which has emphasized cell performance improvements, and (2) to establish a prototype production capability. Capital expenditures, independent research and development funds, and DOE contract cost-sharing have been invested. This investment has provided not only a prototype capability for space CIS cells but a terrestrial CIS submodule prototype production capacity of 8.4 kW_p/yr. Boeing's business strategy during this period of investment has been based on the identification of an interim market for thin–film solar cells in space applications, both defense and commercial. We believe that the long-term potential for the terrestrial PV market exceeds that of the interim market and, as

outlined in the DOE 5-year plan, that the commercial development of interim markets is crucial to the health of the PV industry.

Our prior cost analysis of the production process described in §2 below, based on the technology and equipment currently available at Boeing's Power Systems Development Lab (PSDL) in Renton, Washington, indicated that the currently achievable cost still far exceeds that which is necessary to make PV a viable competitor in the utility power generation market. The analysis conducted in the course of this contract and presented herein of the near- and intermediate-term cost of manufacturing CIGS modules utilizing large-scale inline deposition technology shows that dramatic cost reductions can be anticipated once the development of the required manufacturing equipment is completed. The DOE 5-year plan goals of 15% module efficiency and 30 year lifetime at ~$50/m^2 costs will most likely be achieved by the further development of large-scale manufacturing equipment for $CuIn_{1-x}Ga_xSe_2$ thin–film modules.

We anticipate that by the first decade of the 21st century the photovoltaic industry within the energy sector of the world's economy will resemble the current air transportation industry within the transportation sector. Solar cell module manufacturers will be distributed regionally throughout the world, just as airlines are today. The economic impetus for this dispersion of production is the reduction of product transportation costs to the end users. Just as Boeing is, today, one of the few major manufacturers of the aircraft that enable the airline industry to exist, there will be only a few major manufacturers of the means of producing solar cell modules. Domestic industry and the DOE must cooperate to develop, commercially exploit, and continuously improve the *photovoltaic module manufacturing **equipment** industry* in order for photovoltaics to become and remain a major source of export revenue for the United States.

We believe the greatest obstacle to the successful application of CIGS technology to module production is the high cost associated with the development of manufacturing equipment for the large scale production of CIS and CIGS cells. The development of inline deposition systems for the high-volume manufacture of CIGS modules under the aegis of the PV Manufacturing Initiative represents an opportunity for the Department of Energy, Boeing, and its subcontractors to create a partnership to ensure the domestic production of CIGS modules, the most promising technology for the dramatic reduction of photovoltaic power generation cost.

2. CURRENT CIS SUBMODULE MANUFACTURING TECHNOLOGY

The currently implemented technology at Boeing for the manufacture of CIS submodules has been based on the direct scale-up of laboratory processes developed under either IR&D or prior SERI contracts. The risk of such an approach is quite low, but as will be shown below, fundamental changes are necessary to enable production of submodules at costs which will make them a competitive source of terrestrial electrical power in the future.

2.1. CURRENT CIS SUBMODULE DESIGN

Pilot line equipment is currently installed in the Boeing Aerospace & Electronics' PSDL with a projected annual terrestrial CIS prototype capacity, subsequent to the completion of process scale-up, of 8.4 kW_p . The equipment is tooled for 2 inch square substrates for the fabrication of CIS solar cells for space applications. Most of the tooling is also available for the larger 4 inch square glass substrates needed to fabricate the prototype terrestrial submodule design as shown in figure 2.1-1.

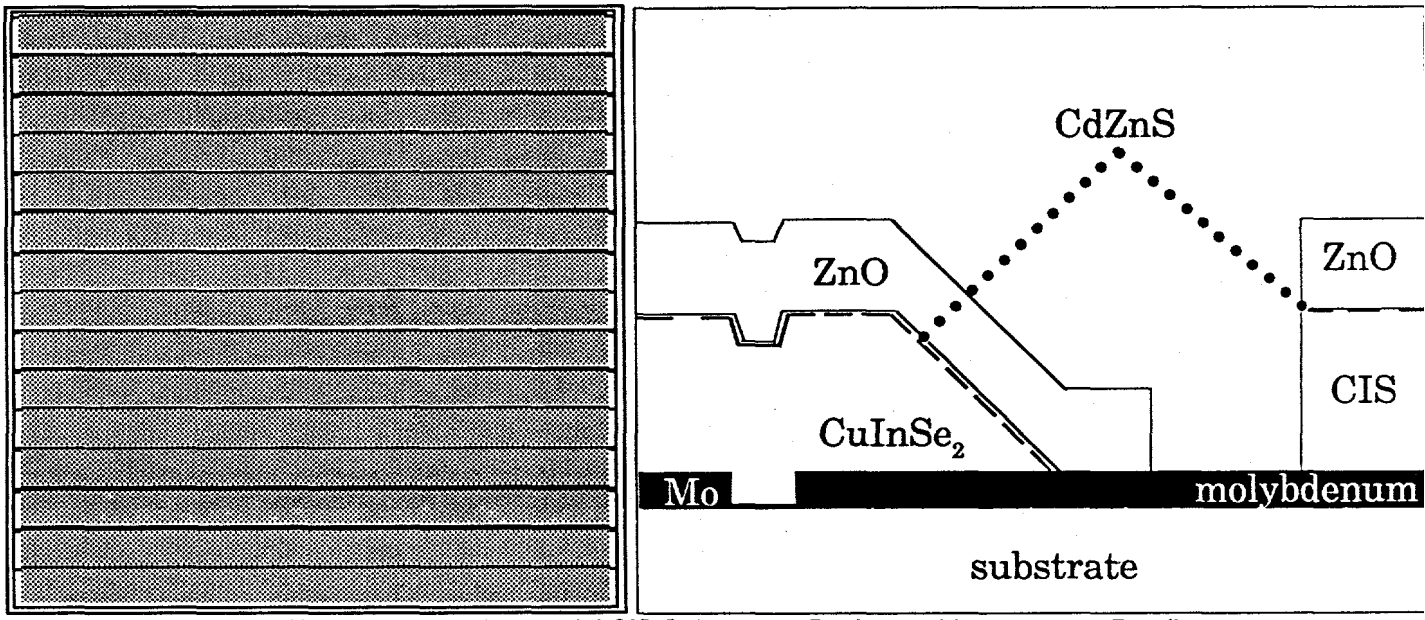

Figure 2.1-1, Terrestrial CIS Submodule Design and Interconnect Detail

2.2. MANUFACTURING PROCEDURE FOR THE CURRENT SUBMODULE DESIGN

A manufacturing procedure to fabricate the submodule design shown in figure 2.1-1 is shown schematically in figure 2.2-1. The procedure consists of nine independent batch processing steps. The Boeing Company is reliant on no other companies or sources for the implementation of this procedure other than suppliers of the utilities and consumable raw materials used in the constituent processes of the procedure.

Terrestrial CIS Submodule Fabrication Procedure Outline

Figure 2.2-1: Terrestrial CIS Submodule Fabrication Procedure

Current Molybdenum Deposition Process: Cleaned glass samples are loaded into a CPA inline sputtering system and pumped into the 10^{-6} torr range. The pallet size is 12" by 12" and holds either 36 substrates that each measure 2" by 2" or 9 substrates that each measure 4" by 4", or one 12" by 12" substrate. The substrates are then moved through a quartz lamp heater zone to remove the water vapor. The chamber is allowed to pump to $3x10^{-7}$ torr. Argon is then introduced into the chamber and the glass is sputter etched for a period of 2 minutes. The substrates are again heated by passing through the heat zone and the pressure in the system is again reduced to less than $3x10^{-7}$ torr. Argon gas is then introduced and Mo is DC-sputtered at ~3kW. The target is 4.75" by 14.875" by 0.25", 99.95% pure and is manufactured by TOSOH SMD,Inc. The film resistivity is 100 mohm/square or less for a one micron thick film. With the present deposition conditions ,the system is able to produce a minimum of bowing due to the deposition process or stress in the Mo. A 2" by 2", 4 mil thick substrate will bow less than 15 mil under these conditions. The amount of bowing is determined by sliding the substrate under its own weight between parallel glass panels sloped at 45 degrees from horizontal.

Current Molybdenum Etching Process: Our Mo etching process is quite simple. After laminating, exposing, and developing the desired pattern with dry-film photoresist, we etch with a commercial etchant containing phosphoric, acetic, and nitric acids. Etching is performed at 55±5°C for ~30 seconds (this etchant evolves hydrogen, and the bubbling stops when the exposed Mo film has been removed). Etching is immediately followed by a quench in heated DI H_2O. Substrates are then rinsed in flowing DI H_2O for ~1 minute, and blown dry in N_2. The dry-film photoresist is then stripped and the substrates rinsed again.

General Description of CIS ($CuInSe_2$) & CIGS ($CuInGaSe_2$) Deposition Process: The polycrystalline CIS thin–film is prepared in a batch type chamber by coevaporation of the three elements onto a heated metallized substrate. The properties of the deposited film are largely determined by the Cu to In ratio in the film. Films with high Cu/In ratios (>0.95) are low resistivity, large grain, *p*-type material exhibiting (112) preferred orientation. Low ratio films(<0.85) are high resistivity, small grain, *n*-type material with little of the desired (112) preferred orientation. Boeing invented a bilayer process involving both of these films types and this process has been utilized throughout the PV field to prepare CIS films which are capable of yielding high efficiency solar cells. In the Boeing two layer process, the first film is deposited with Cu/In fluxes adjusted to produce a low resistivity, large grained deposit (i.e., high Cu/In ratio). After 2/3's the deposition time has elapsed, the Cu rate is reduced to approximately 70% of its initial value and maintained at the lower level for the remaining 1/3 of the deposition cycle. Along with the Cu rate change, the substrate temperature is increased by 100°C. If deposited by itself, a CIS film prepared under the low Cu rate conditions would be high resistivity, *n*-type material. However, due to extensive interdiffusion of the two layers during deposition, the final film resulting from the bilayer process is a densified film with moderately high resistivity, *p*-type conduction, ~1-micron grain size with preferred (112) orientation, and no detectable composition gradients.

Because of the high sensitivity of the CIS film to the Cu/In ratio, control over the deposition fluxes and the areal uniformity across the substrate are critical to the success of the deposition process. Boeing has adopted EIES rate controllers with unique sensor head mounting configurations for control of the fluxes and specialized vapor source or substrate geometries to achieve composition uniformity. In contrast to the high Cu/In sensitivity, the CIS films prepared by co-evaporation are found to not be strongly influenced by the Se deposition rate. The general procedure is simply to use Se rates of 2-3 times those required for stoichiometric material and have the excess Se re-evaporate from the heated substrate/growing CIS film. The vaporization sources for the Cu and In materials are typically Mo or W boats with an alumina barrier to contain the liquid materials. Furnace sources with BN crucibles and electron-gun sources are, however, also in use. Source temperatures are estimated to be in the 1300°C range for Cu and 900°C for In. Selenium is evaporated from Ta boats or SS crucibles (directly heated) and the rate controlled with quartz crystal-based deposition controllers. Source temperatures are in the 225-250°C range. CIGS films are prepared by processes identical to those described above for CIS. The difference, of course, is the addition of a fourth vaporization source for Ga and a controller for its deposition rate. A furnace source with a BN crucible (~1100°C) and a second EIES unit are used to satisfy these requirements. In the batch chamber, the compositional uniformity with the four element codeposition is achieved by source placement and rotating substrates. It should also be noted that the addition of the Ga requires the use of substrate temperatures 100°C higher than those for CIS and it has been observed that the Ga is not very mobile in the CIGS films. Thus, unlike CIS, composition gradients normal to the film surface are possible and can be applied to prepare advanced devices with increased cell efficiencies.

Current CdZnS Deposition Process:

Aqueous-chemical deposition solutions:

(1) $(Cd,Zn)Cl_2$ solution

0.0042M $CdCl_2 \cdot 2(1/2)\ H_2O$

0.00105M $ZnCl_2$

0.013M NH_4Cl

(2) Thiourea solution

0.0417M $(NH_2)_2CS$

(3) NH_4OH solution

1.875 M NH_4OH

Water bath temperature: 85°C

Mix solutions (1)+(2)+(3), (1):(2):(3) = 200:200:1

CIGS or CIS coated substrates are put into the reaction vessel with the solution preferably flowing parallel to the substrate surface. CdZnS is deposited on all surfaces, including substrates and the container walls (heterogeneous reaction) and is also precipitated in the solution (homogeneous reaction). The substrates are left in the solution until after the reactants are depleted,

about 15 minutes. Substrates are next removed from the reaction vessel and are ultrasonically agitated and rinsed in DI water and dried in dry N_2 gas.

The Cd content in 200cc of solution (2) is 0.0944g which could produce 0.121g CdS. This quantity would be enough to coat more than 5 square feet with 50 nm thickness of CdS film. However, the competition of the CdS precipitation in the solution and the CdS deposition on the substrates make the usage of the Cd less than ideal. Currently, we coated 8, 2x1 inch substrates on both sides and the beaker wall in a 500cc beaker containing 200cc each of solution (1) and (2). The total coating area is about 0.5 sq.ft.. The collection efficiency of Cd is only about 10%. To increase the efficiency, future designs would emphasize maximization of the module front-surface coating area in a given volume of reaction tank with the constraint that the solution be adequately agitated.

Current Semiconductor Etching Process: Our CIGS/CdZnS bilayer etching process is quite simple. After laminating, exposing, and developing the desired pattern with dry-film photoresist, we etch with a commercial etchant containing bromine dissolved in alcohol. Etching is performed at 35±5°C for ~60 seconds . Etching is immediately followed by a quench in heated alcohol. Substrates are then rinsed in flowing DI H_2O for ~1 minute, and blown dry in N_2. The dry-film photoresist is then stripped and the substrates rinsed again.

Current ZnO Sputtering Process: The ZnO films are deposited in an inline system by RF magnetron sputtering onto the moving substrate in an argon or oxygen/argon atmosphere. Just before deposition of ZnO onto the sulfide-coated substrates, the substrates are baked at low temperature in air for 5 min. The substrates are nominally at room temperature, no deliberate substrate heating is used. The ZnO target is doped 2% by weight Al_2O_3. The ZnO used is deposited in two steps to form a high resistivity/low resistivity bilayer. First a thin (90 nm) high resistivity layer is deposited using a relatively high oxygen content ambient. A thick (640 nm typical)low resistivity layer is then deposited using pure Argon as the ambient. The film resistivity is controlled by the O_2/Ar ratio in the sputtering gas. Film thickness is controlled by substrate speed.

Typical deposition conditions are:

RF power: 1 kW at 13.56 MHz for target size of 14.875 in by 4.75 in

Total pressure: 5×10^{-3} torr

We use cylinders of pure Argon and a mixture of 5% oxygen and 95% argon in order to control the oxygen partial pressure more accurately. We do not have calibrated gas flowmeters, but the gas flow depends on the deposition system anyway; e.g. the chamber size and pumping capability.

The resistivity of the ~640 nm thick low-resistivity layer is about 28 ohms/square. The resistivity of the high-resistivity layer is not measurable in its normal ~90 nm thick device thickness, but substantially thicker (~640 nm) test layers made under the same nominal conditions show a resistivity of 100-150 ohms/square. Films deposited on glass are smooth, exhibiting no visible haze. Optical transmittance of the bilayer ZnO film structure varies between 80-90% over the wavelength range of 400-1200 nm.

Current ZnO Etching Process: As for molybdenum, our ZnO etching process is also quite simple. After laminating, exposing, and developing the desired pattern with dry-film photoresist, we etch with a solution of dilute hydrochloric acid. Etching is performed at room temperature for ~30 seconds. Etching is immediately followed by rinsing in flowing DI H_2O for ~1 minute, and blown dry in N_2. The dry-film photoresist is then stripped and the substrates rinsed again.

2.3. MANUFACTURING EQUIPMENT FOR THE CURRENT SUBMODULE DESIGN

All of the processes required to fabricate the structure described in §2.1 by the procedure described in §2.2 have been demonstrated on a laboratory scale, and are compatible with the pilot line processing equipment identified in figure 2.3-1 below. That equipment which is already of an inline design and currently in use is identified by bold type. The importance of inline equipment will become apparent in the subsequent submodule cost analysis discussions.

Process Description	Procedure	Equipment
Substrate Cleaning	Batch ultrasonic detergent/rinse	Heated ultrasonic baths & rinsers
Mo Contact Deposition	DC magnetron sputtering	**1ft^2 substrate capacity inline sputtering system**
Mo Patterning	Dry-film PR, wet chemical etch	Laminator, exposure system, spray developer & stripper, heated batch etch tanks
CIS Deposition	Elemental co-deposition	Large-capacity planetary evaporator
CdZnS Deposition	aqueous chemical deposition (~400 Å)	Heated batch chemical processing tanks
Semiconductor Patterning	Dry-film PR, wet chemical etch	Laminator, exposure system, spray developer & stripper, heated batch etch tanks
ZnO Deposition, O_2 bake	RF magnetron sputtering	**1ft^2 substrate capacity inline sputtering system**
Subcell Isolation Patterning	Dry-film PR, wet chemical etch	Laminator, exposure system, spray developer & stripper, heated batch etch tanks
Deshunt & Submodule Test	Electrical	Solar simulator, power supplies, multimeters, and computer

Figure 2.3-1: CIS Prototype Submodule Production Synopsis

2.4. COST ANALYSIS OF SUBMODULES BY CURRENT TECHNOLOGY

We have estimated the manufacturing cost of prototype CIS submodules fabricated by the procedure delineated in fig. 2.3-1 on the pilot line equipment currently located in the Boeing PSDL. We used the actual book value of that equipment (using 5-year amortization and straight-line

depreciation), the actual facilities lease expense, the suppliers' published prices for the raw materials purchased in the quantities required to support this throughput, and realistic assumptions regarding fully fringe-benefit-burdened labor rates, scheduled and unscheduled downtime, scheduling inefficiencies, and yield to calculate approximate production costs. All calculations are in 1990 dollars and assume a three-shift operation. These estimates do not reflect the actual price of pilot line production at Boeing because such an estimate would be based only on direct material requirements and labor expenses fully burdened with overhead expenses for the entire Boeing Aerospace & Electronics organization. This analysis represents the cost of such production activity in the context of an independent accounting profit-and-cost-center. The net yield of 10% efficient, 100 cm^2 CIS submodules from glass in to tested submodule out is assumed to be 65%. The resulting cost for unencapsulated submodules is $71 each or $\$78/W_p$. Although not yet competitive for terrestrial applications, the PSDL CIS pilot line capacity is well matched to Boeing's anticipated near-term requirements for the interim space market. Our current plan is to accelerate the manufacturing technology development for larger-scale applications while simultaneously pursuing lower costs.

The analysis shown in figure 2.4-1 identifies the major cost elements that must be reduced to make this technology applicable to DOE's low-cost terrestrial solar energy goals. From the cost-by-category breakdown it is apparent that drastic reductions in labor/part must be achieved: ***automation is mandatory***. This is particularly true if the U.S. PV industry is to compete successfully with offshore competitors who enjoy significantly lower labor rates. The second largest contribution to the overall cost by category analysis is capital depreciation. Further detail reveals that dominant component of this cost in the Boeing PSDL CIS pilot line process is depreciation of the CIS planetary evaporator. Development of ***inline CIS deposition equipment*** and processes with a higher ratio of throughput to capital cost is the solution. The contribution of raw materials cost is greatly inflated by three factors. First, ***batch processing is wasteful*** compared to continuous processing (no waste recovery was assumed); second, the collection efficiency of equipment intended for deposition onto small substrates is poor compared to equipment intended for ***larger substrate size***; and third, raw materials cost on a per unit basis could be dramatically reduced by ***much higher production volume***.

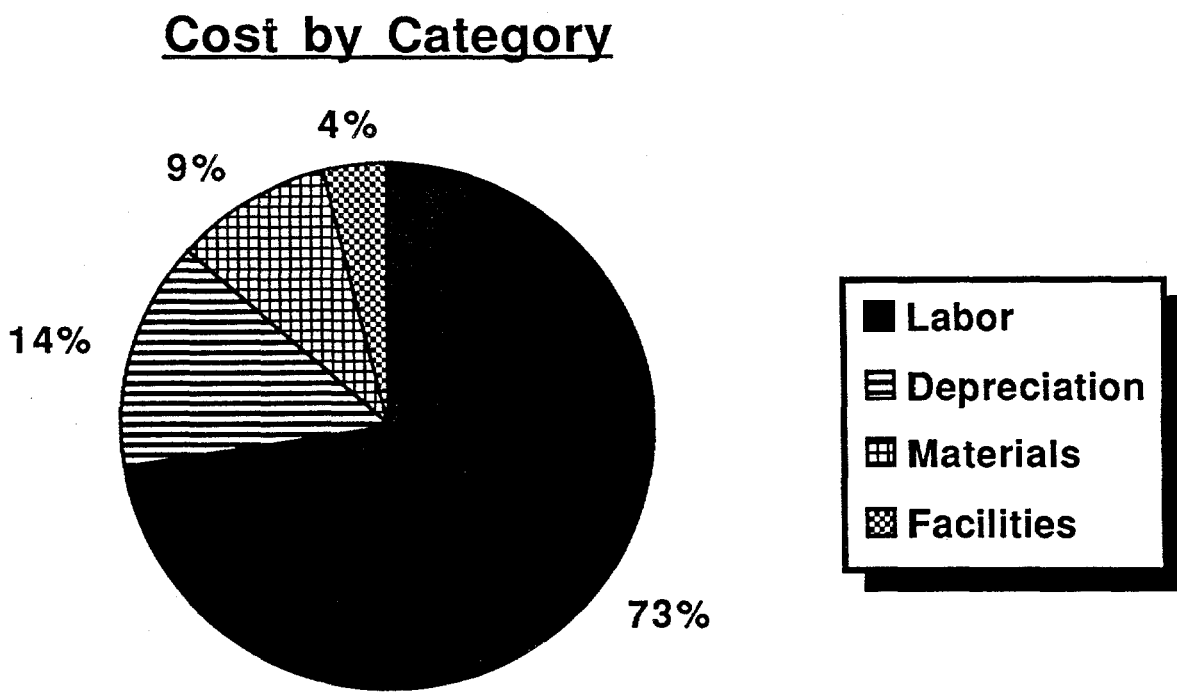

Figure 2.4-1: Pilot Line CIS Submodule Cost Breakdown by Category

Further insight into effective cost-reduction strategies can be obtained from the analysis of cost by process step (figure 2.4-2). The three dominant cost elements, jointly comprising 55% of the total, are the deposition of Mo, CIS, and ZnO. Although both the Mo and ZnO deposition systems are inline systems capable of deposition onto $1ft^2$ substrates, neither has automated cassette load/unload capabilities. Hence they are essentially batch systems, and this fact is reflected in very high labor costs associated with those steps in the Boeing PSDL CIS pilot line process. We have analyzed the cost of the Mo deposition step in the process with the assumption that the commercially available cassette load/unload was added. In this scenario, the cost contribution of this process step drops to $1/4^{th}$ of its prior value; to less than 5% of the total submodule cost. Even this is not the limiting case because automated cassette load/unload merely makes the batch size larger. ***Continuous processing, waste recovery and larger deposition zone width*** would each contribute to even further cost reductions. These conclusions are reflected in our discussion of manufacturing processes that can lead to improved performance, reduced manufacturing costs, and significantly increased production in §3.

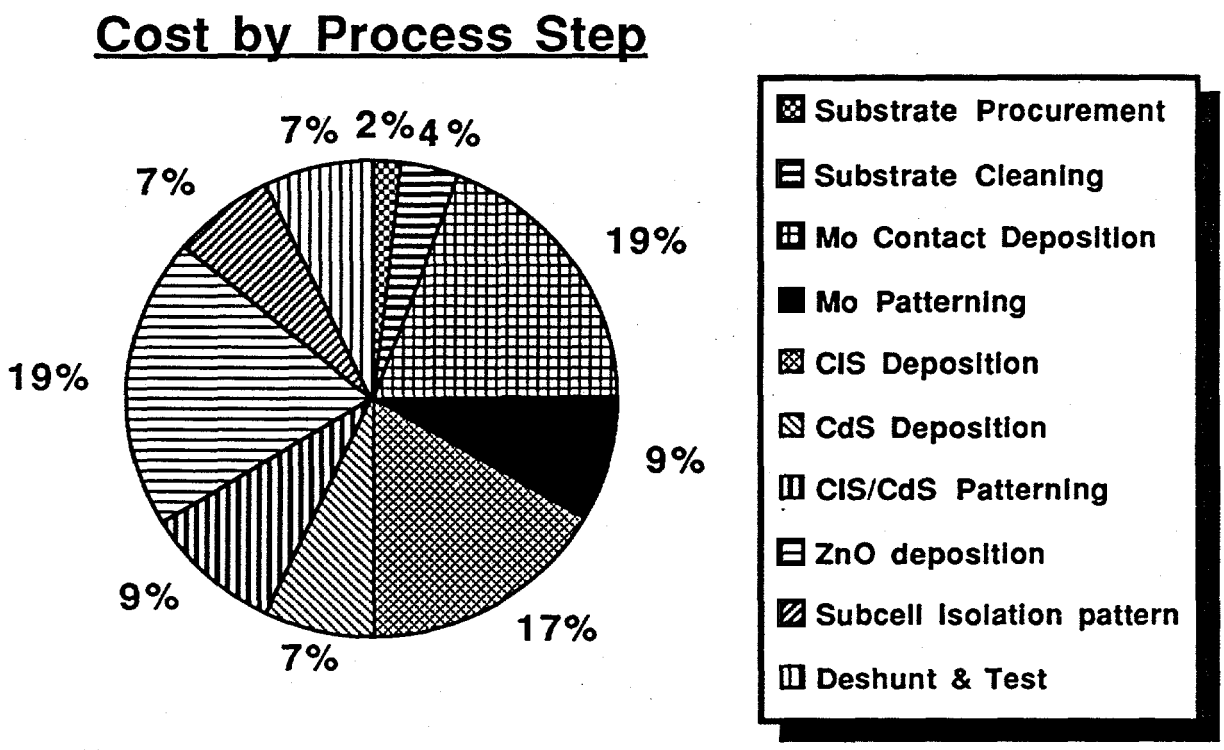

Figure 2.2-2: Pilot Line CIS Submodule Cost Breakdown by Process Step

The three patterning steps in the Boeing PSDL CIS pilot line process jointly comprise 25%, or one quarter of the total submodule cost. These processes are all based on dry-film laminated photoresist, optical photomask exposure, and wet chemical develop, etch and strip processes similar to those commonly used in the printed circuit board (PCB) industry. No automation is currently used in these processes and, as a consequence, their expense is dominated by labor costs in this analysis. Significant cost reductions could therefore be achieved by automation as is the case in large-scale PCB manufacturing operations throughout the world. We believe that the great number of substeps, handling and transfer operations, and, ultimately, the costs of the photolithography materials themselves, will not permit this technology to achieve the long–term cost goals. The alternative which we envision will be discussed in §3.

3. PROPOSED CIGS MODULE MANUFACTURING PROCEDURE

Our prior research and development work on CIS and CIGS technology has been guided mostly by the goal of maximizing cell efficiency. In contrast our technical plan for commercializing thin–film CIGS modules is guided by the minimization of power generation capacity cost, measured in $\$/W_p$. It is crucial to remember in this delicate process of judging tradeoffs between performance and cost the experiences of the PV industry in the '80s: a product which is cheap but inefficient, such as α-Si:H, cannot necessarily compete successfully with the more expensive but efficient incumbent technology, crystalline silicon. The strategy underlying our technical plan can be correctly viewed both as the adaptation of continuous inline α-Si:H production equipment to the requirements of CIGS module manufacturing in order to increase module efficiency to levels comparable to those of crystalline silicon, and as the adaptation of our current CIGS fabrication process to the requirements of continuous inline processing of much larger substrates in order to reduce module cost. Boeing's prime lower tier subcontractor, GSI, has successfully demonstrated continuous inline production plants for amorphous silicon PV modules and believes strongly that similar inline plants for CIGS can be manufactured.

Boeing and GSI began the PVMaT program with a bilateral exchange of information about our respective device fabrication processes, under the auspices of a two-way proprietary information agreement. Specifically, Boeing provided to GSI a description of the envisioned device structure and the current processes used for the deposition of each of the device layers and for the patterning of those layers as required to implement that structure. GSI in turn provided Boeing a detailed description of their current α-Si manufacturing process and equipment. Significant evolution in the pilot line and module design has taken place as a direct consequence of technical capabilities currently implemented in GSI's α-Si inline manufacturing system which are applicable to CIGS module production with appropriate changes to both the α-Si processes and the CIGS module design.

Our evaluation of potential CIGS manufacturing procedures suggest that nonsemiconductor equipment for the production plant can be very similar to that used for α-Si:H production and will require only minor changes. Existing α-Si inline system modules potentially applicable to CIGS manufacturing include automated system controls, glass substrate heating and transport mechanisms, initial glass cleaning, x-y translation tables for laser scribing, gas handling and injection manifolds for CVD, DC magnetron sputtering, patterning and chemical etching (modified chemistry for molybdenum), selective interconnect process, and panel testing. These specific elements of GSI's current technology have been selected for incorporated into our CIGS module development plan. A schematic outline of the procedure which we intend to implement in the Prototype Inline CIGS Production Plant is shown in figure 3.0-1.

Prototype CIGS Module Inline Process

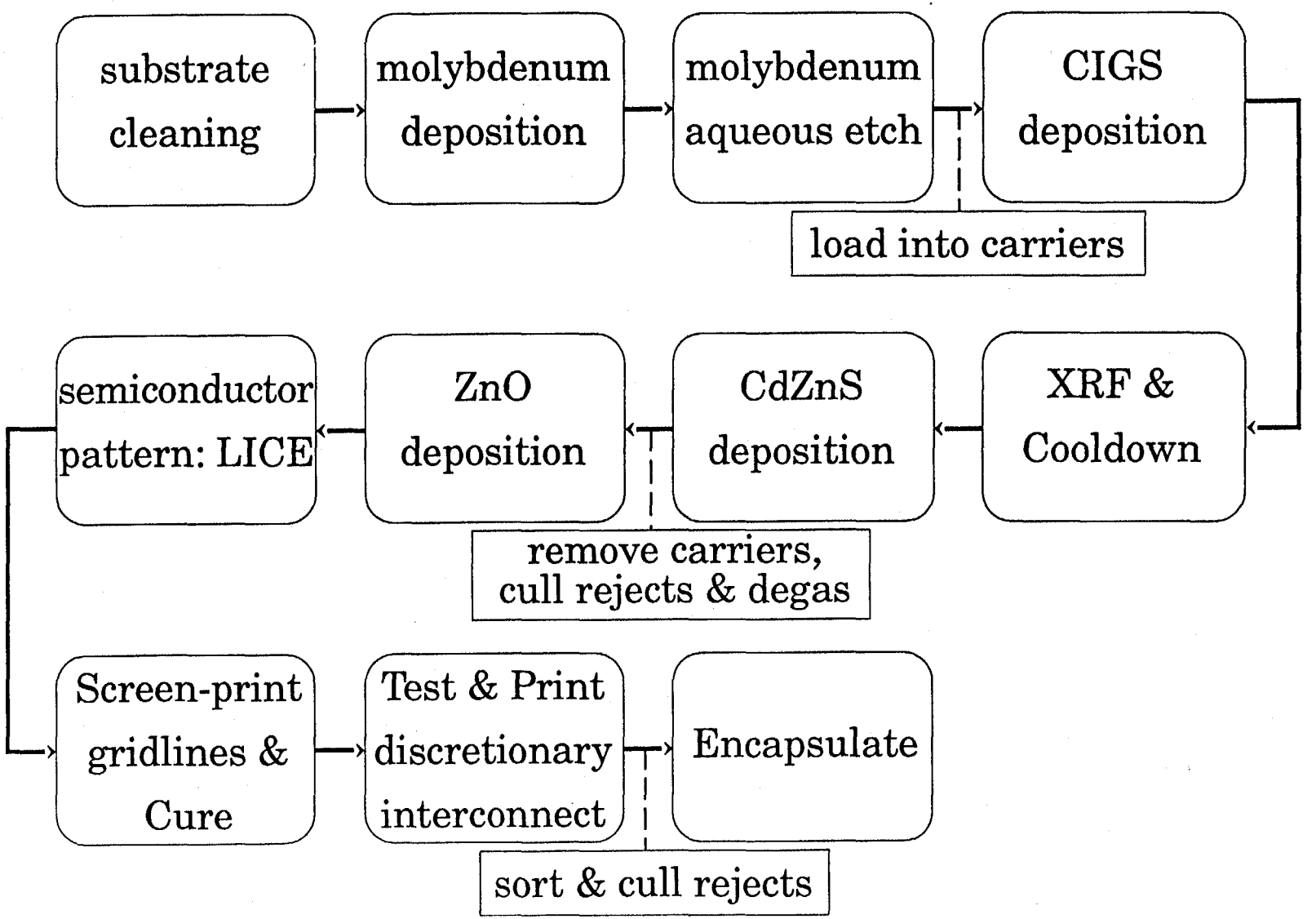

Figure 3.0-1: Prototype Inline CIGS Production Procedure

The *Prototype* Inline CIGS Production Plant analyzed in the course of this contract and described in this document is the next logical step in the further development of CIGS module manufacturing technology. It represents an *interim* step towards the ultimate achievement of the *goals of DOE's Five Year Plan*, which our analysis suggests *can be achieved by* scale-up and refinement of the Prototype Plant to what we shall call the *Full-scale* Inline CIGS Production Plant, as discussed below.

The Prototype Inline CIGS Production Plant will implement the procedure outlined in figure 3.0-1 on 1 foot by 4 foot submodules, six of which will be combined into each 4 foot by 6 foot module. The prototype plant will: utilize the latest available technology–rotating anode magnetron sputtering for the deposition of molybdenum and zinc oxide contact layers and the LICE semiconductor patterning processes recently developed by Boeing and its collaborators; provide a platform for the demonstration of large–area co–evaporation of the CIGS active absorber layer; and rely on technology adapted from GSI's existing α-Si inline systems for the patterning of molybdenum and the screen-printing of gridlines and discretionary interconnect busses. Incorporation of the discretionary interconnect technology is particularly important to insure the achievement of high yields in the prototype plant because of the absence of *a priori* information about the areal densities of deleterious defects. Cost analysis of modules produced by the Prototype Inline CIGS Production Plant is presented in §4 which shows that given conservative assumptions regarding yield and performance, the 2–4 MW_p/year product of the prototype plant can be produced for a competitive price at the time of its availability. Figure 3.0-2 shows the design of the CIGS submodule designed for the procedure shown in figure 3.0-1.

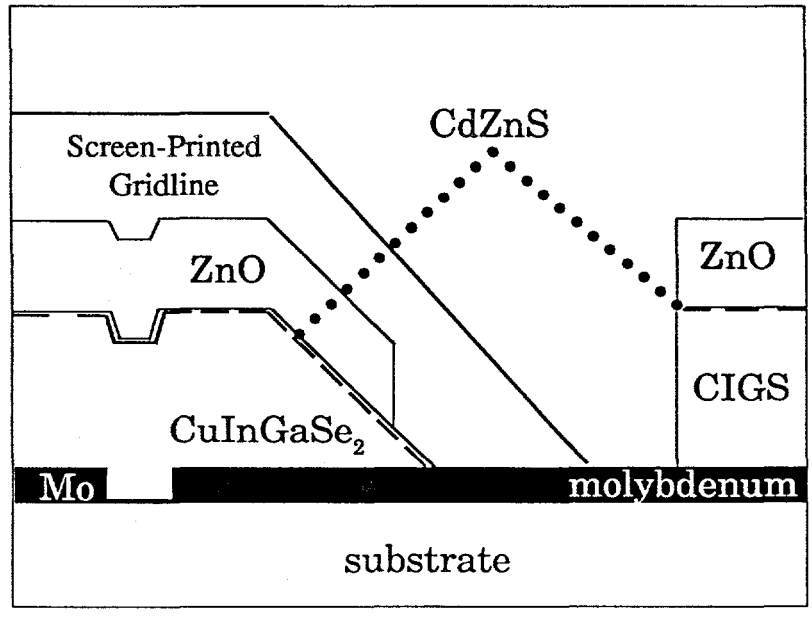

Figure 3.0-2: Prototype CIGS Submodule Interconnect Design Detail

The Full-scale Inline CIGS Production Plant represents the subsequent step in our CIGS module manufacturing technology development plan. It is based on the procedure outlined in figure 3.0-3 performed directly with 4 foot by 6 foot substrates. In addition to this further submodule size scale-up, the proposed procedure reduces the materials costs for module fabrication by eliminating the single most expensive cost element from the prototype product: gridlines. The resulting decrease in optimum cell width in the submodule design permits the direct monolithic integration of sufficient numbers of cells on each submodule to generate output voltages high enough for direct connection of each module to the input of an inverter–the ideal product for central utility systems. Our cost analysis for the Full-scale Inline CIGS Production Plant, also presented in §4, shows that it has the potential of achieving the cost goals of the DOE's Five Year Plan and of the Renewable Energy and Energy Efficiency Technology Competitiveness Technology Act of 1989 at its projected full-capacity production levels of 10-17 MW_p/year.

The cost of electrical power generated by PV modules ultimately depends both on the module specific cost ($/$W_p$) and the module lifetime. The intrinsic stability of thin–film cells based on CIS has been amply confirmed by independent testing by SERI, but achieving the DOE's goal of a 30-year module lifetime will also require protection of the cells from potential extrinsic causes of degradation. Certainly the most ubiquitous problem for all PV technologies is corrosion due to long-term exposure to water vapor. Both the prototype and full-scale CIGS module production plant will implement a Boeing proprietary module encapsulation technology invented prior to this contract, which will enable the cost-effective fabrication of hermetically sealed modules without any polymeric encapsulant and with minimal optical reflection losses that could degrade module performance. This proprietary technology is anticipated to provide a solution to this generic problem with potential applicability to modules based on other cell technologies.

The procedures for production of CIGS modules in both the prototype and full-scale plants can be grouped into five basic steps, each of which is performed by a single production line. Together with support facilities to provide their utility requirements and an automated control system to coordinate parts flow between them, these five lines constitute a CIGS module production plant. These five basic steps are: front end substrate preparation, CIGS deposition, CdZnS deposition, device processing, and back end module processing. Each of these steps, the process technology for each step in the prototype and full-scale plants, and a description of the equipment lines for process execution will be discussed separately and in detail in the following subsections.

Figure 3.0-3: Full-scale Inline CIGS Production Procedure

3.1. FRONT END: SUBSTRATE PREPARATION

In both the prototype and full-scale CIGS module production plants the front end substrate preparation step consists of substrate cleaning, molybdenum deposition, patterning of the moly film to define the separate cell back contacts, and a final cleaning to prepare the substrates for the subsequent CIGS deposition step. Boeing and GSI have designed a single automated inline system to accomplish these processes serially and at high throughput rates. In both the prototype and full-scale systems the substrates are transported along their narrower axis (1 foot and 4 feet, respectively) which dictates that the system width accommodate the longest dimension of the submodules, either 4 feet or 6 feet, respectively.

The first subsystem is a commercially available glass washer which cleans the incoming substrates. The substrates are automatically transferred from the exit of this system into the load lock chamber of the molybdenum deposition subsystem. This technology is currently implemented in GSI's α-Si:H inline system and represents almost no risk or uncertainty.

The molybdenum deposition subsystem is the first of four inline vacuum systems incorporated into each module production plant. All of the four vacuum systems are designed modularly from two types of common vacuum chambers: vertical and horizontal transport chambers. Reliance on construction techniques which utilize modular chambers significantly reduces their production cost and increases the flexibility of the systems, enabling the system design to be modified to incorporate process improvements or modifications at less cost. The current baseline design of the molybdenum deposition subsystem is comprised of 6 modular horizontal-transport inline chambers: load lock, preheat, sputter-etch, 2nd preheat, molybdenum sputtering (downward), and a cooldown/exit lock. This design permits replication in detail of our current laboratory process, but it may not be necessary to incorporate the sputter-etching step into the final production process. If this is possible the sputter-etching chamber and one preheat chamber could be eliminated, further reducing capital costs.

Prior Boeing-funded studies of large-scale molybdenum sputter deposition systems have been based on the assumption that conventional planar magnetron sputtering targets would be utilized. The cost analysis of production based on this assumption has revealed two problems. First, in order to achieve adequate throughput and continuous system uptime, a large number of targets and power supplies are required—five are required to provide the prototype line system a continuous 6-day operational lifetime. Second, only a small fraction of a conventional planar magnetron sputtering target can be utilized because of uneven target erosion. This low "utilization efficiency", typically ~25%, combined with modest flux collection efficiencies (~47% for ±10% uniformity on a 4-6 foot width) imposes another significant cost penalty. Our new design incorporates a recently developed cylindrical rotating cathode technology, which offers higher utilization efficiency (~75%), higher collection efficiency (~75%), and longer target continuous operation lifetimes. The net result is a cost-effective solution to the problem of high-volume, large-area molybdenum deposition.

The final component subsystem in the front end substrate processing line is a pattern etcher comprised of three sequential stations. First a high precision, high speed screen printer is used to apply a maskant used to block exposure of the molybdenum film to the etchant in those areas where it must remain. Next, the panel is subjected to an aqueous chemical etch solution which removes the unmasked molybdenum film. The etch solution is recirculated to maximize its utilization efficiency, and total etch time is ~1 minute. Finally, a substrate cleaning station after the etcher is used to remove the maskant material from the glass, thus readying it for the next step in our CIGS module manufacturing procedure.

3.2. CIGS DEPOSITION

The process most likely to provide these large–area, low-cost CIGS modules is the one giving the best possible combination of performance and manufacturing yield. Boeing has pioneered such a process in the development of high-efficiency CIS and CIGS cells using a batch process based upon co–evaporation of the elements to prepare the thin–film absorber. The co–evaporation method offers significant advantages in terms of film quality, material composition flexibility and the potential for lower temperature CIGS growth. We fully recognize that the demonstrated batch processes will not provide the manufacturing costs and throughput needed for a successful terrestrial solar cell production operation. However, we believe those goals can be best achieved by the adaptation of successfully demonstrated continuous inline production equipment originally developed for α-Si:H to the co–evaporation of CIGS thin–films onto heated, large–area substrates. Our approach to continuous inline co–evaporation, described in detail below, promises to circumvent reproducibility problems associated with the batch process and speed the pace of module performance improvement. Current evidence suggests that competing techniques for the formation of CIS films such as selenization do not permit adequate control over the film growth kinetics to enable low-temperature formation of high quality, higher performance CIGS materials; or the controlled, high-yield implementation of advanced device structures incorporating gallium composition gradients. These factors translate into enhanced cell efficiencies and lower manufacturing costs.

In both the prototype and full-scale CIGS module production plants, the metallized glass substrates exiting the final station of the front end substrate preparation line would be placed into vertical carriers which after passing through a load lock chamber, are heated and automatically transported to a high vacuum chamber containing a vaporization source module where they would be continuously coated with the CIGS film material. The vaporization sources would be configured in a line so that the substrates would be uniformly coated during their passage through the deposition zone along their longer axis. The continuous deposition process is capable of very large substrate throughputs and low operational costs. Furthermore, since the width of the deposition module and the number of modules can both be scaled, there is considerable room for greatly enhanced production capacity when scaling from prototype to full-scale production.

There are, obviously, several major problems which must be addressed and overcome before this deposition concept can actually be realized. These include line source designs capable of uniformly coating a moving substrate, source designs capable of producing films with uniform final compositions as well as the bilayer composition gradient during deposition, designs consistent with achieving these film properties over extended periods of time, control methods to maintain the film composition, source/chamber configurations capable of high collection efficiency for the evaporating material and for simulating the conditions found necessary in the batch evaporation chambers for preparing high quality material, and chamber/transport system designs capable of operating at the high substrate temperatures currently needed for CIGS film deposition. We believe we now have developed solutions to each of these problem areas and, with the completion of the defined developments, the successful inline production of CIGS cells by co–evaporation will be demonstrated. Each of these solutions will now be described.

In order to achieve uniform film deposition across the moving substrate surface, a line vaporization source oriented normal to the direction of substrate motion has been designed. The source would consist of a long heated tube containing apertures where the vaporized source material would be emitted. The tube would be connected to a large, heated reservoir containing the source material. The temperature of the reservoir would primarily be used to control the vapor pressure of the source material (and, subsequently, deposition rate) while the tube temperature would simply be maintained at a sufficiently high value to prevent condensation of the source vapor. Both the reservoir and the tube would be surrounded by at least two radiation shields to reduce heat losses and power consumption. We have used computer programs to analyze the vapor flux emission from the tube apertures and to arrive at designs providing acceptable coating uniformity on a 1 foot wide substrate. Wider substrates could be analyzed as the need arises. In these models, we have assumed the emission distribution from each aperture to be that of a small area source (Knudsen's cosine law). We recognize that there are errors in making this simplified assumption but these should not significantly alter the projected results and would be corrected once the experimental distribution has been determined for an actual source aperture. Initial calculations showed that excellent uniformity could be achieved($\pm 1\%$) across the substrate surface directly over the line source by using a source to substrate distance of 8 inches, three apertures, an 8 inch spacing between the apertures, and having the area of the center aperture 75% of the outer two. However, when the film thickness distribution was determined by integrating the contribution from each aperture while the substrate passed through the deposition zone, a five aperture source with a source-to-substrate distance of 7 inches was required to achieve the same uniformity. In this case, the middle apertures were located 5.2 inches from center and the outer two apertures 8 inches from center. A plot of the calculated integrated, normalized film distribution predicted for this source configuration is shown in figure 3.2-1.

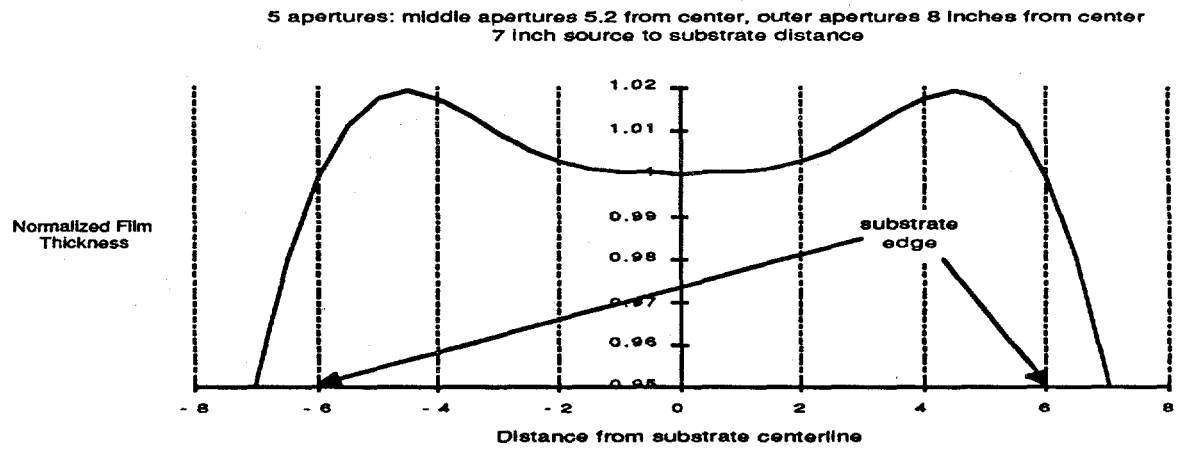

Figure 3.2-1: Integrated, normalized Thickness Distribution of film deposited by Line Source with Distance from Source

The deposition zone referred to above is defined by a deposition shield aperture whose length (parallel to the direction of substrate travel) was determined by impingement angle restrictions for proper film growth (<45°) and whose width (vertical axis) was determined by the substrate size or chamber considerations (1 foot for the prototype line and 4 feet for the full-scale). For the data presented in figure 3.2-1, a 14 inches deposition aperture length was utilized. By allowing the deposition aperture length to increase to very large values, the total material emitted from the source may be estimated. A comparison of this value to that of the material collected on the substrate makes it possible to estimate the collection efficiency for the deposition process. An example of this type of computation is shown in figure 3.2-2 for the five aperture source.

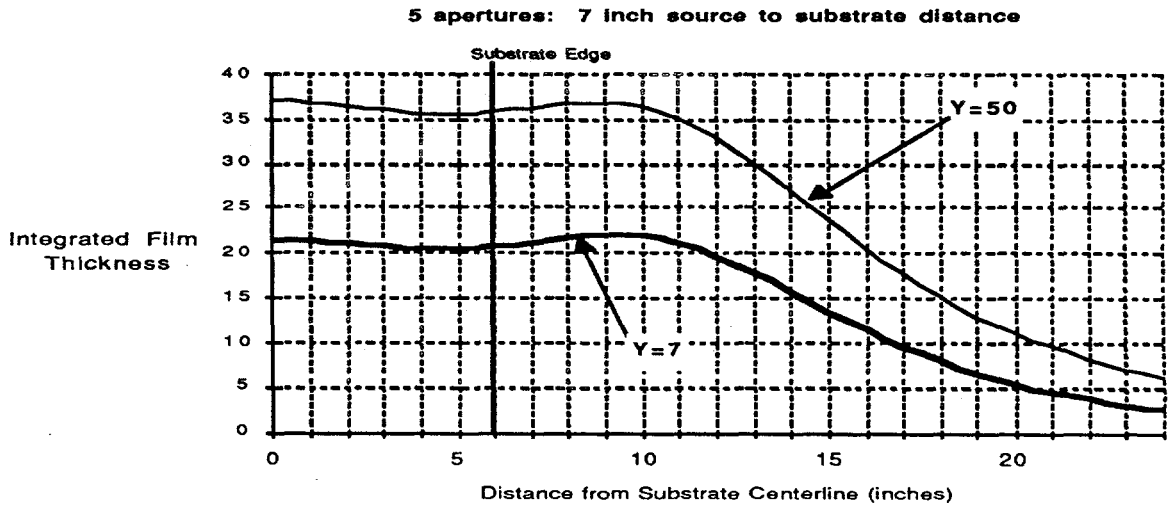

Figure 3.2-2: Integrated Thickness Distribution of film with Distance from Line Source

In this figure "Y" refers to half the deposition aperture length. Using Y–values of 7 inches and 50 inches , a collection efficiency of 35% was calculated. By combining the collection

efficiency data with minimum film thickness and maximum deposition rate requirements, it was then possible to determine aperture areas, source temperatures, source power, material consumption rates, and deposition line (substrate) speed. The results of the calculations have been specific source structures whose parameters appear to be quite reasonable and achievable and have been applied to complete the manufacturing cost analysis for the CIGS–based cells.

As part of the design activity relating to the sources for the coevaporation process, two general line source types were considered. First was a line source for each individual material; i.e.: Cu, In, Ga, and Se. For CIS material, it was possible by appropriately locating the Cu & In tube source to simulate the required bilayer deposition conditions on the moving substrate and achieve acceptable film thickness uniformities. However, in view of the need to deposit CIGS material, the stringent composition uniformity requirements, and the desirability for higher line speeds, a second source configuration was adopted for the three critical metal elements. The configuration is that incorporating a sparger or secondary vapor mixing chamber. The sparger would be connected to the tube line source and would be fed from reservoirs containing the three source materials. A rate limiting aperture would be located between each reservoir and the sparger. This aperture and the reservoir temperature would be utilized to control the relative amounts of each elements. The vapors would be mixed in the sparger chamber and then the mixed composition would be emitted from the apertures contained in the long tube source. The sparger chamber and the tube source would be independently heated from the reservoirs and would be maintained at sufficiently high temperatures to prevent deposition of any of the three materials.

By mixing the three vapors, the problem of compositional uniformity across the substrate would be avoided. Film composition control then would become a matter of selecting the proper rate-limiting aperture and maintaining a constant reservoir temperature. Providing the reservoir heating and temperature sensing/control methods are correct, only long term drift would be anticipated. Corrections to the slowly responding reservoirs would be made according to the post deposition film compositional analysis/process control methodology discussed below. The reservoirs would further be sized to provide 144 (=6x24) hours of continuous operation before requiring replenishment. Essentially, they would also be located externally to the deposition chamber by the use of valves and other vacuum hardware so that the replenishment would not necessitate venting the deposition chambers.

The adoption of the sparger source configuration for the bilayer CIGS film preparation would best be implemented by two deposition modules (one for each composition) in the manufacturing line. A heating module separating the two modules would provide for the substrate temperature ramping which is part of the established CIGS bilayer deposition process. While the sparger configuration line source would be used for the three metals, a simple line source, again with five apertures would be used for Se evaporation. In this case two Se line sources would be used with each positioned 4 inches from the center of the deposition shield aperture and 6 inches from the substrate. This arrangement results in a reasonably uniform Se flux with values of approximately 2x those required for stoichiometric material.

One final but important point regarding the inline chamber design is that of substrate heating, temperature resistant transport systems, and prevention of sagging in the low cost glass substrates. This would be accomplished by utilizing a GSI system design incorporating vertical substrate transport with the glass held by its top edge with proven transport mechanisms used to hold glass during high-temperature annealing. The line sources for the CIGS deposition would, of course, also be oriented vertically but this would not change the deposition analysis discussed above and would, in fact, be a more attractive configuration.

Various strategies for control of the selenide deposition sources have been explored. We have concluded it is necessary to divide the source control into a short time constant temperature or rate control of the source itself and an in-situ monitoring of the film composition to correct for drift in the film composition and thickness if necessary. The feasibility of using X-Ray Fluorescence (XRF) as the in-situ monitoring method has been explored, and while complex to implement, there do not appear to be any insurmountable obstacles to this approach. There are, however, several system constraints to be placed on the design of this system. These include,

1) The location of the detection apparatus.

2) The measurement time constants, feedback mechanism, and logistics.

Each of these constraints will be discussed separately along with the reasoning which led to the particular constraint, followed by a discussion of any additional XRF features that would enhance its versatility in this application.

1) The XRF detection apparatus must be located outside of the CIGS deposition region.

This constraint is based upon three interacting properties of the deposition system and measurement apparatus requirements that are mutually exclusive in a system. 1) The geometry of an XRF instrument requires that both the excitation source and the detectors be relatively close to the sample site and for proper stability must be cooled, 2) the extreme reactivity of the selenium overpressure and reaction byproducts present in the deposition chamber tend to react with and deposit on any exposed surface, and 3) the substrate temperature in the deposition regime is over 350°C. These properties combine such that having this type of detection system located in this deposition chamber is impractical at this time and possibly damaging to the XRF apparatus itself. Therefore, the XRF apparatus must be isolated from the deposition chamber in terms of temperature, pressure, and reaction products which implies either differentially pumped chambers or a load-lock arrangement. An additional result of this constraint is the necessary addition of specialized transport mechanism to the sample measurement chamber and an x-y stage at the XRF site.

2) The measurement control system requires a division of the source control to a two time constant system.

Because the initial substrates to be used are individual 1'x4' glass plates, constraint 1) requires that the XRF detection system determine the composition of one sample in the measuring chamber while another sample is being deposited. This would require that the XRF be detecting on substrate #1, while #2 is being deposited, and presumably #3 would be in the deposition zone before any feedback from the measurements is made. The XRF feedback

mechanism would be through an algorithm which 1) takes a reading of the $CuIn_{1-x}Ga_xSe_2$ composition, 2) executes an algorithm which would calculate the source temperature changes required to optimize the deposition parameters, 3) communicate to the source temperatures controllers the required temperature ramps, 4) continue to measure the substrate for CIGS nonuniformities which would shut the line down.

Several companies have expressed interest in pursuing the implementation of such a system and we have had samples measured by these companies to determine the feasibility of the measurement of CIS and CIGS thin films. Initial feedback from one of these companies indicates that the total measurement time that is required to obtain the 0.1% accuracy on the order of 30 seconds using a scanning spectrometer. Shorter measurement times are available using a simultaneous measurement spectrophotometer but at a significant increase in cost. We contend that measurement times on the order of 30 seconds are sufficiently fast for this application because the XRF measurement is required for monitoring the long time drifts of the thermal sources resulting in the subtle changes of film composition. The relative ease of measuring these thin films to the accuracy of 0.1% lies in the fact that the sample contains large percentages for each of the elements throughout the thin film stack. An additional bonus from using an X-ray excitation source over the electron beam excitation source is that it provides a molybdenum back contact signal in the emission spectra. This detection will presumably allow a direct measurement of the thickness of the CIS or CIGS thin film. In conclusion, the use of an XRF spectrometer inline thin film detector will allow the best method of monitoring the fabricated thin film composition and thickness to provide feedback to the thermal sources to correct for long term thermal drifts which change the film composition. The XRF detector must be placed in a separate measurement chamber due to the nature of the measurement and the reactive species. Future development may permit the placement of this XRF detector in the deposition region, provide direct feedback to the thermal sources and eliminate the constraint to the ex–situ feedback measurement scheme.

The overall CIGS deposition line configuration in both the prototype line and full scale scenarios consists of 9 inline vertical vacuum chambers. Those chambers are an entry load lock, two preheat chambers, a CIGS 1st layer deposition chamber, an isolation chamber, a CIGS 2nd layer deposition chamber, a cooldown chamber, an XRF chamber, and an exit load lock. Within the constraint of reasonably achievable deposition rates for high quality CIGS, our analysis has predicted that to minimize total module cost two such CIGS deposition lines operating in parallel are required to optimally utilize the throughput capacity of the front end and back end lines in both the prototype line and full scale CIGS module production plants.

3.3. CdZnS DEPOSITION

A large–area, high-yield CIGS deposition process is necessary, but not sufficient, for the economical fabrication of thin–film CIGS modules. Another key process required is a high-yield, high-throughput technique for the deposition of ultrathin (~300Å) conformal layers of the $Cd_{1-y}Zn_yS$ heterojunction contact onto the CIGS prior to ZnO deposition. Our space cell process is the electron-beam evaporation of the semiconductor, but this technology is incapable of achieving

the degree of thinness required for high performance without resulting in excessive pinholes, which lead to shunting. Scale-up of the aqueous chemical deposition technique developed by Boeing and utilized in our record CIGS cells is feasible. Insufficient yield data are currently available to assess whether that technology will be able to satisfy the needs of a production process. This process is critical to device performance and yield, hence we considered it prudent to evaluate another alternative with a high probability of success. Specifically, organometallic chemical vapor deposition (MOCVD) is capable of producing highly uniform, conformal coatings over large areas. Coupled with its amenability to scale-up, this might make it well suited to the cost-effective growth of thin (~300Å) uniform heterojunction contact layers of $Cd_{1-y}Zn_yS$ on CIGS. We have analyzed this supposition with the assistance of our subcontractor ATM. The result of the technology evaluation is presented below and the economic analysis will be presented in §4, where we have analyzed the cost/performance/yield trade–offs in the context of the prototype line.

3.3.1 Aqueous Chemical Deposition of the $Cd_{1-y}Zn_yS$ Heterojunction Contact Layer

Our major concern regarding the aqueous chemical deposition of CdZnS layers, as we mentioned in the proposal, are the throughput, chemical utilization efficiency, integration of the wet process with the vacuum process in an inline production plant, and yield of the process. After a careful preliminary studies of the manufacturing process under this contract, we conclude the design and system integration issues can be solved. To accommodate a predetermined throughput requirement the size and number of reaction vessels can be designed for either an inline or a batch aqueous deposition system. In order to maximize the chemical utilization efficiency, the ratio of the tank volume to the coating area needs to be optimized. For instance, in an inline system multiple parallel tracks to carry the substrates through the tank should be designed. Such a design will not only maximize the utilization efficiency but also increase the throughput. A special casette will be designed to hold the substrates back–to–back to prevent sulfide deposition on their backside. The wet chemical process in the present designed inline system does not create any problem. A manual station to change the fixtures for carrying the substrates is presently designed in between the vacuum and wet processes. In the future a robotic system can be used to replace the manual system to further reduce the cost. Pinholes in the thin sulfide layer of the large area module which lead to shunting are a major concern. Insufficient data are currently available to assess this problem. However, if the problem arises, the sulfide layer thickness can be increased by either increasing the chemical concentration in the solution or multiple dipping to reduce the pinhole problem. Increasing sulfide thickness will decrease the blue response and hence the efficiency. A compromise between the efficiency and the yield would will be sought which minimizes the module power cost.

3.3.2 MOCVD of the $Cd_{1-y}Zn_yS$ Heterojunction Contact Layer

The objective of the CdZnS MOCVD process module is to deposit a uniform thin (300–400 Å) heterojunction contact layer of $Cd_{1-y}Zn_yS$ onto polycrystalline copper indium diselenide ($CuInSe_2$) and copper indium gallium diselenide ($CuIn_{1-x}Ga_xSe_2$). The process must occur at low temperature (<200°C) and be cost effective. The key technical issues include control of both the gas phase and surface chemistries. Innovative reactor design and process controls will be required to implement the chemistries on a manufacturing scale.

- The low growth temperature required will necessitate careful selection of reagents and growth techniques to allow growth at the desired temperature.
- The surface to be coated will be very rough with hills and valleys approximately 1000-2000 Å in size. Deposition of a uniform, conformal coating only 300-400Å in thickness on such a surface will require extremely uniform nucleation of the CdZnS layer.
- To keep the costs within desired limits the process must be designed to minimize the cost of organometallic reagents.

The proposed process will be based on the use of Atomic Layer Epitaxy (ALE). Atomic layer epitaxy (ALE) refers to the growth of an epitaxial layer one atomic layer at a time through the use of self limiting reactions. First proposed in 1980 for ZnO, it has been extended to the growth of both II-VI and III-V semiconductors. The sequence of steps for ALE growth of e.g., ZnS, involves exposing the surface of the growing epitaxial layer alternatively to the Zn and S precursor molecules. The zinc species, which may be a partially pyrolyzed precursor molecule, is adsorbed until q_{Zn} (q = fraction of surface sites occupied by zinc) is unity. The reactor is purged, followed by the introduction of the S source, normally H_2S, which reacts with the adsorbed zinc layer, covering it with one monolayer of SH. Following a purge, this cycle is repeated. The chemistry involved is obviously complex and at least partially heterogeneous. This technique has been used to grow ZnSe at 200-275°C [Yoshikawa, A.; Okamoto, T.; Yasuda, H,; Yamaga, S.; Kasai, H. *J. of Crystal Growth* **1990**, *101*, 86]

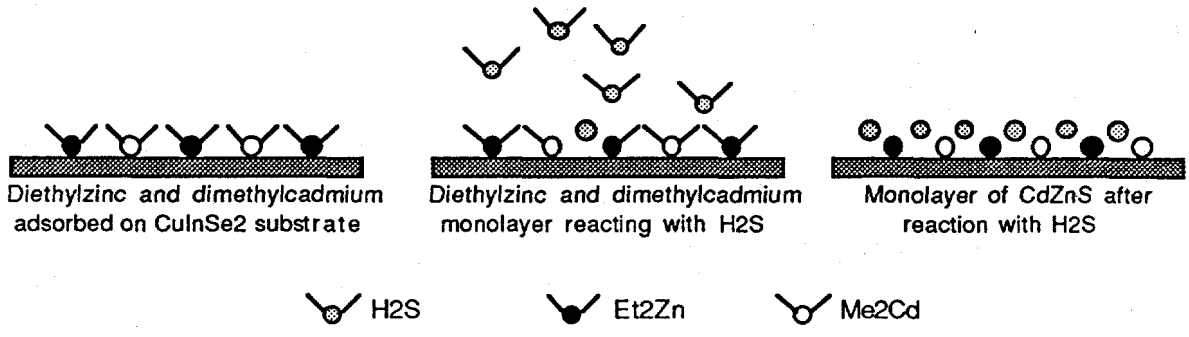

Figure 3.3.2-1 ALE deposition of CdZnS from dimethylcadmium, diethylzinc, and hydrogen sulfide.

In addition to facilitating growth at low temperatures use of ALE is expected to aid in achieving uniform nucleation on the extremely rough substrate. This is due to the relatively long

surface migration time available to the Group II species before they are exposed to molecules of the Group VI reagent. ALE also avoids the problem of gas phase pre-reaction which is common in the growth of II-VI compound semiconductors by MOCVD. The Group II and Group VI reagents are not present in the gas phase at the same time therefore they cannot pre-react. ZnSe layers grown by ALE are superior in quality to those grown by conventional MOCVD, a difference which has been attributed to the absence of pre-reaction [ibid].

Approximately 100 cycles will be needed to achieve the desired thickness. Each ALE cycle is anticipated to be 20–40 seconds long; thus 35–70 minutes would be needed per substrate to deposit the desired coating. In production, based on a nominal track speed of 3.6 inches/min and a substrate length of 48 inches the available time is 13 minutes. The deposition will therefore need to occur in five different chambers, based on our standard modular chamber size. The substrate will receive twenty growth cycles in each chamber. One gas manifold can be used to service all five chambers. Air actuated valves in conjunction with a process logic controller will be used to distribute reagents to the desired chambers at the appropriate times.

We expect that dimethylcadmium, diethylzinc, and hydrogen sulfide will be the preferred reagents. The group IIB alkyls react readily at room temperature with any proton source, including hydrogen sulfide (Figure 1).

$$H_2S + R_2M \longrightarrow 2\ RH + MS \qquad M = Cd,Zn$$

Figure 3.3.2-1 Reaction of Group IIB metal alkyls with hydrogen sulfide.

The dimethylcadmium and diethylzinc gas streams will be mixed in the manifold and then allowed to pass into the reactor. After a purge the hydrogen sulfide flow will be allowed into the reactor. The dimethylcadmium and diethylzinc molecules which are adsorbed on the substrate surface will react with the hydrogen sulfide to form the desired CdZnS layer.

Two major questions must be answered. First, can the CdZnS layers be deposited in the required uniformity and purity? Second, can the process be made cost effective? Process cost variables have been analyzed and the results are presented in §4. The efficiency of reagent utilization and strategies for minimizing reagent costs are addressed specifically by the choice of an ALE growth process. The design of production reactors to incorporate nucleation and growth process variables and transfer of the technology to manufacturing represent represent a significant development activity. Details of our plan to do so will be presented in detail in §5.

3.4. DEVICE PROCESSING

In both the prototype and full–scale CIGS module production plants the device processing step consists of zinc oxide deposition and patterning of the semiconductor films. However in the prototype line, these processes are sequential and the patterning serves to isolate the individual cells from one another. In the full–scale line there are two patterning steps, one each before and after the zinc oxide deposition. The first patterning process isolates the CIGS and CdZnS bilayer into distinct devices and the second isolates the subsequently deposited blanket zinc oxide layer into

distinct interconnects bridging the front contact of each cell to the molybdenum back contact of one of its neighbors, thereby connecting them in series. In the prototype line this series interconnection is created selectively during the back end module processing in order to provide a discretionary interconnect capability whose goal is to improve the yield during the inline technology development phase of CIGS module commercialization.

The device processing line for the prototype plant consists of 5 horizontal modular vacuum chambers: a load lock, a ZnO sputtering chamber, an isolation chamber, a Laser–Induced Chemical Etching (LICE) chamber, and an exit load lock. The full scale device processing line consists of 7 somewhat larger horizontal modular vacuum chambers: a load lock, a LICE chamber for patterning CIGS/CdZnS bilayers, an isolation chamber, a ZnO sputtering chamber, another isolation chamber, a LICE chamber for ZnO patterning, and an exit load lock. In both cases the entry load lock is automatically fed from a conveyorized IR oven which bakes the CdZnS-coated CIGS films in air in order to optimize their photovoltaic performance. This effect has been widely described in the CIS literature since its original discovery by Boeing researchers. In the baseline case where the CdZnS is deposited by aqueous chemical deposition, the IR oven also serves to dehydrate the films prior to their introduction into vacuum.

The zinc oxide deposition process is based on the reactive sputtering of a 2% aluminum-doped metallic zinc target in an argon/oxygen atmosphere utilizing essentially the same rotating cylindrical cathode magnetron sputtering technology proposed for the deposition of molybdenum in the front end substrate deposition process (cf: §3.1.) The power levels which can be utilized for sputtering of ZnO are somewhat lower than those achievable for molybdenum due to its lower melting point and its greater tendency to arc. Nevertheless, the economics of this approach are far superior to those of conventional planar magnetron reactive sputtering, RF magnetron sputtering from oxide targets, or MOCVD of ZnO. The potential risk of this approach is that substantially lower power levels than those assumed in the economic analysis of §4 will be required in order to mitigate thermal and/or ion bombardment damage effects on the underlying junction. This could result in a need for multiple cathodes which would increase the cost. Sensitivity analysis in §4 will show that the cost impact of this change to the baseline assumptions would be minimal.

In collaboration with another laboratory, Boeing has demonstrated a high-rate Laser-Induced Chemical Etching (LICE) process for etching CIS. We have already demonstrated complete selective etching of a CIS layer on molybdenum in 12 seconds, and have technical justification for anticipating that this process can be speeded up to between 1 and 3 seconds/cut. The process is inherently parallel, or in other words scanning is not necessarily required. Nevertheless our analysis indicates that the most cost-effective solution will be a combination of scanning and fixed optics. Due to proprietary information constraints between ourselves and the co-developer, specific details of the process cannot be disclosed at this time. For these purposes the process can be described by its throughput, capital cost, maintenance costs, utilities costs, and consumable raw materials' costs.

Our preliminary module design is based on a 41 by 6 cell series/parallel arrangement, requiring 48 cuts/module. Assuming etch times of 2 seconds/cut and translation times of

2 seconds/cut gives a total processing time of 3.2 minutes/module with a laser duty factor of 50%.

Laser maintenance parts are estimated to be $10./operating-hr and consumable utilities costs are estimated to be $0.435/operating-hr. Multiplying each by the operational duty factor of 50% for real-time cost, we get $5.23/hr for utilities and maintenance parts.

3.5. BACK END: MODULE PROCESSING

We believe that there will be a distinct market by the end of this decade for modules specifically tailored to the requirements of central utility power generation, as well as the more conventional market for stand-alone applications. Our module manufacturing systems should accommodate customers for both requirements, however utility customers may have a specific interest in the product variation we propose here: *hermetically encapsulated frameless modules with a longer lifetime* than that of conventionally encapsulated modules. This hermetic edge-sealing technology is the subject of a pending Boeing invention disclosure.

Module encapsulation using this process will require pre-processing of the front module coverglass before its attachment to the module substrate on which the cells have been formed. Incoming glass superstrates should be cleaned. It would be most cost-effective to utilize the same cleaner used for the substrate line since its throughput is adequate and its utilization in the prototype and full scale scenarios is low. After cleaning the superstrate it is exposed on one side only to a chemical treatment for 2 minutes, creating an extremely effective anti-reflective coating, and then dryed before further processing. After this process, a narrow and thin layer of the edge sealant is screen-printed along the perimeter of the superstrate on its etched side and then heated in a conveyorized IR convection oven to the 300-360°C temperature range for at least 20 seconds. The superstrate is then aligned with and mounted onto the substrate under a dry argon blanket, and the perimeter sealed by a lineal process at a scan speed of 2 inches/second.

Total consumable material cost for the process is $0.05/module assuming a 1ft x 4 ft module size. The sealing components themselves are estimated to cost $30K, excluding the x-y table. The superstrate glass need not be exactly the same size as the substrate; indeed the module may be sturdier if the superstrate is somewhat larger.

4. PROJECTED COST OF MODULES

We have computed the manufacturing cost of CIGS modules fabricated by the procedures delineated in figures 3.0-1 for the prototype plant and 3.0-3 for the full–scale plant. We used capital equipment prices jointly developed with our subcontractors GSI and ATM to determine the depreciation expenses incurred (using 5-year amortization and straight-line depreciation) by a module producer who has purchased a turnkey production plant from a module manufacturing equipment company. Materials costs are based on recent purchase prices, published price lists, or suppliers' cost estimates for the raw materials purchased in the quantities required to support this throughput. Realistic assumptions regarding fully fringe-benefit-burdened wage rates and factory labor staffing requirements are used to calculate labor costs. Scheduled maintenance was assumed to require one full day per week plus two weeks for an annual overhaul. Unscheduled downtime, module efficiency and yield at each step of the procedure have been parametrically varied to estimate the potential range of module production and power generation capacity costs. Sets of these variables have been coupled with our best estimates of the probability that they can be achieved at different stages of the technology development. This permits sophisticated risk analysis. All calculations are in 1991 dollars and assume a three-shift operation during net uptime.

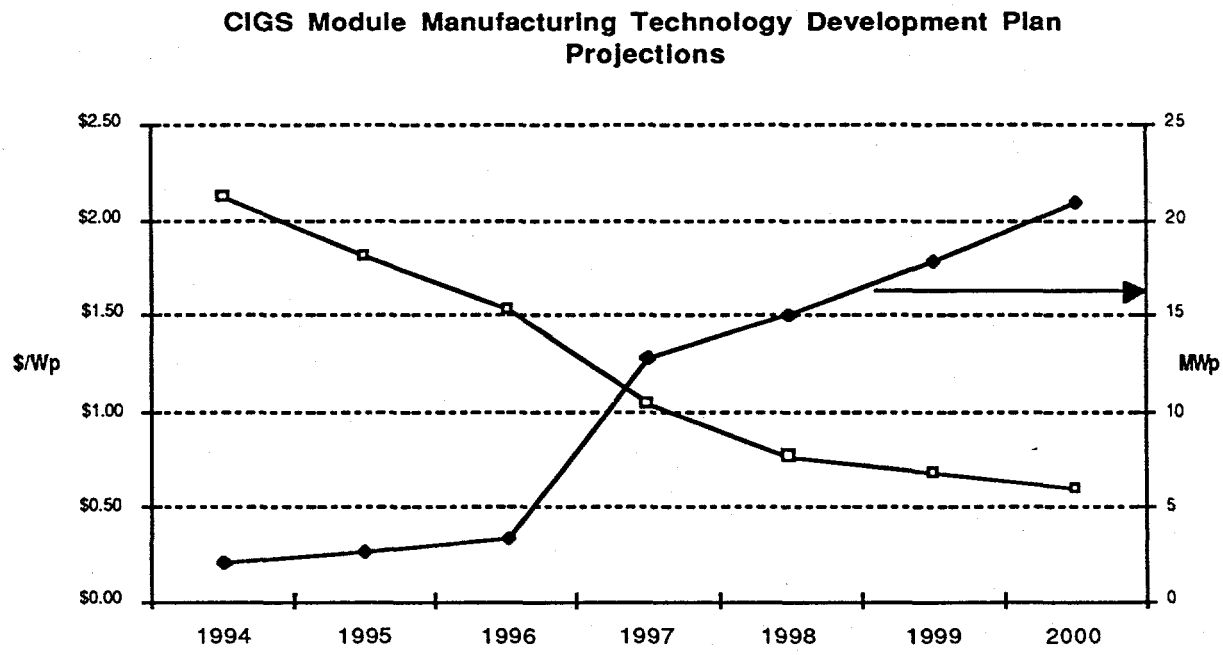

Figure 4.-1: Projected Module Power Cost and Production Capacity

These calculated direct manufacturing costs have been combined with the technology development plan schedule described in §5 to project the module peak power production cost in $\$/W_p$ and the output capacity in MW_p as a function of time between the years 1994 when the

prototype production plant is expected to be first operational and the year 2000 when the first refined, fully developed full–scale production plant achieves its full capacity. A complete tabulation of the parametric assumptions for the calculations at each production level and the resulting cost element breakdowns are contained in Appendix A. We will simply note here that those assumptions are quite conservative, with net yields and uptimes assumed to be only 66% at the beginning of operations and initial efficiencies of only 12%.

Each step of the module manufacturing procedure has been modelled separately and in great detail. Each process step model incorporates process cycle times, variable inline track speeds, adjustable power levels and other relevant adjustable variables, along with fixed equipment design and process constraint parameters, and calculates numerous intermediate dependent variables. The calculated results from these models have used to guide our process and equipment choices to insure that power generation cost ($/$W_p$) is the final determinant figure-of-merit. As a consequence they have been revised numerous times in the course of this contract. Linear programming techniques have been used to maximize the utilization of each process line and to match the throughput capacities of the various steps in each procedure.

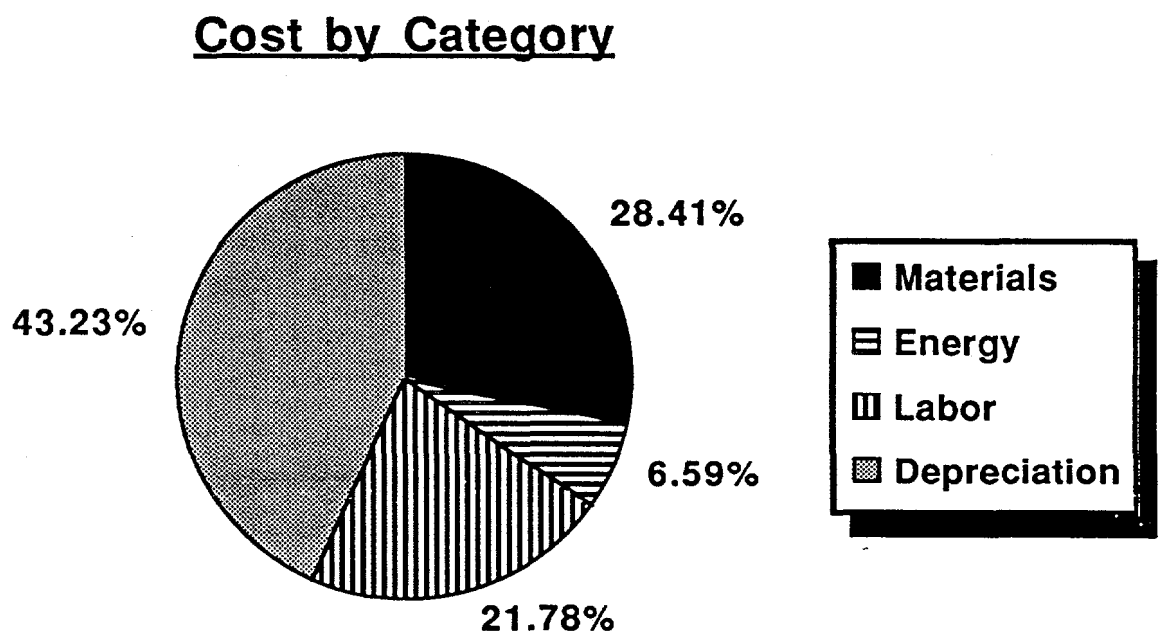

Figure 4.-2: Prototype Inline CIGS Module Product Cost Breakdown by Category

A comparison of this cost breakdown by category for the Prototype Inline Plant with that of the current pilot line shown in figure 2.4-1 reveals a striking reduction in the labor cost per module and an increase in the depreciation and materials expense proportion. Keep in mind that the cost basis for these two breakdowns has been reduced from a level of $78/$W_p$ in the pilot line to

$1.32/$W_p$ in the prototype inline plant's product, *a factor of 60 cost reduction and a factor of 480 output volume increase!* Figure 4.-3 below shows the same cost breakdown for the Full-Scale Inline Plant. Here we see that a further increase in output from 4 to 17 MW_p further reduces the labor expenses, and increases the materials expense proportion, indicating a higher output/capital ratio. The cost basis for the full-scale production case has been further reduced from the pilot line levels to **$0.57/$W_p$**. We note that the *recurring* expenses after the full depreciation of the initial capital investment are represented by the sum of the non-capital categories: different accounting assumptions regarding depreciation and amortization could significantly reduce the projected total cost. The lower limit is represented by these recurring expenses, and amount to **$0.31/$W_p$**.

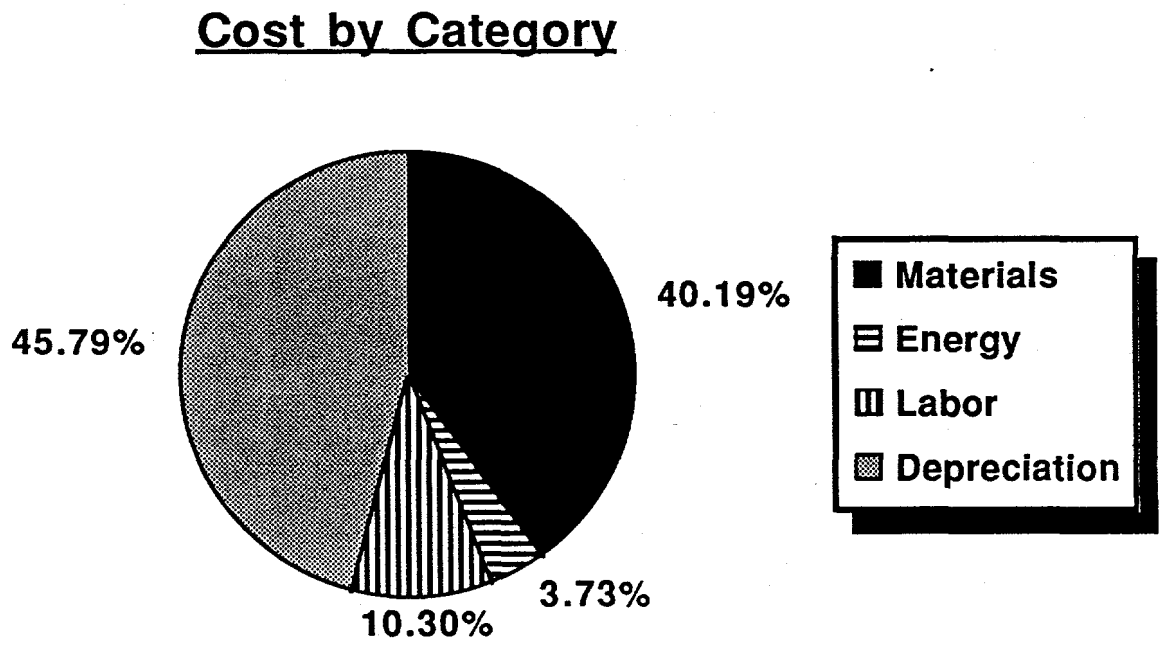

Figure 4.-3: Full-scale Inline CIGS Module Product Cost Breakdown by Category

The next chart, figure 4.-4, shows a further breakdown of the materials cost content of each module by layer or category. Note that glass is the dominant expense category, constituting over half of the total materials cost. The next most expensive category is the CIGS layer containing copper, indium, gallium, and selenium. This category is dominated by the indium and gallium costs.

We also present in figure 4.-5, a breakdown of the full–scale production cost by step in the manufacturing procedure. This data reveals that the most expensive step in the process in the deposition of CIGS, followed by the front end and back end processing (each of which includes glass costs for substrate and superstrate, respectively.) Comparison with figure 4.3, above, shows that the expense of the CIGS deposition step includes significant contributions from both materials and capital.

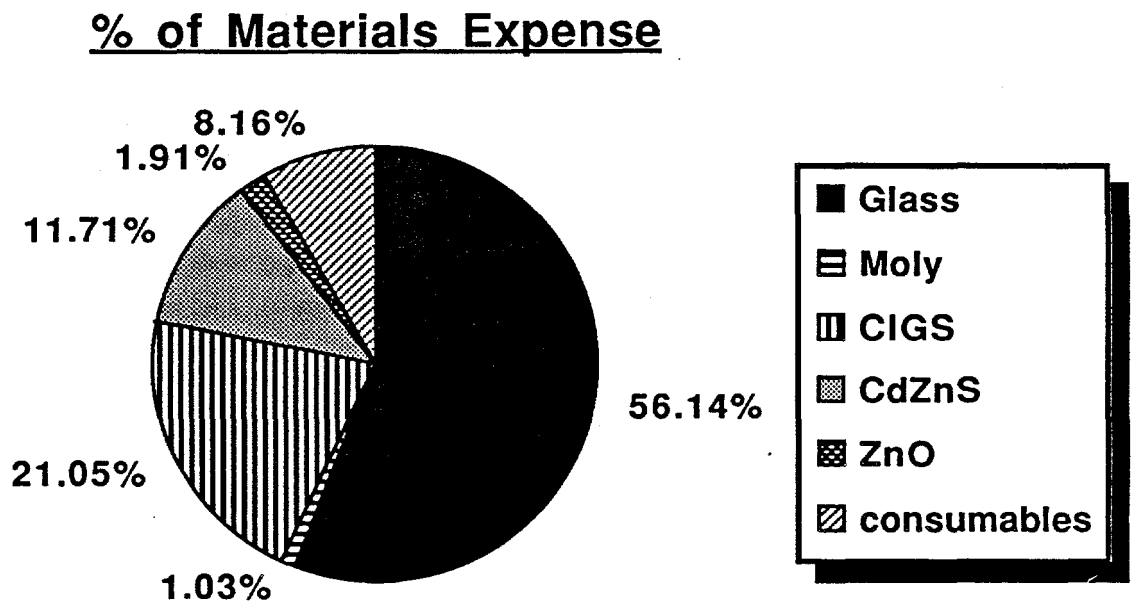

Figure 4.-4: Full-scale Inline CIGS Module Material Cost Breakdown by Layer

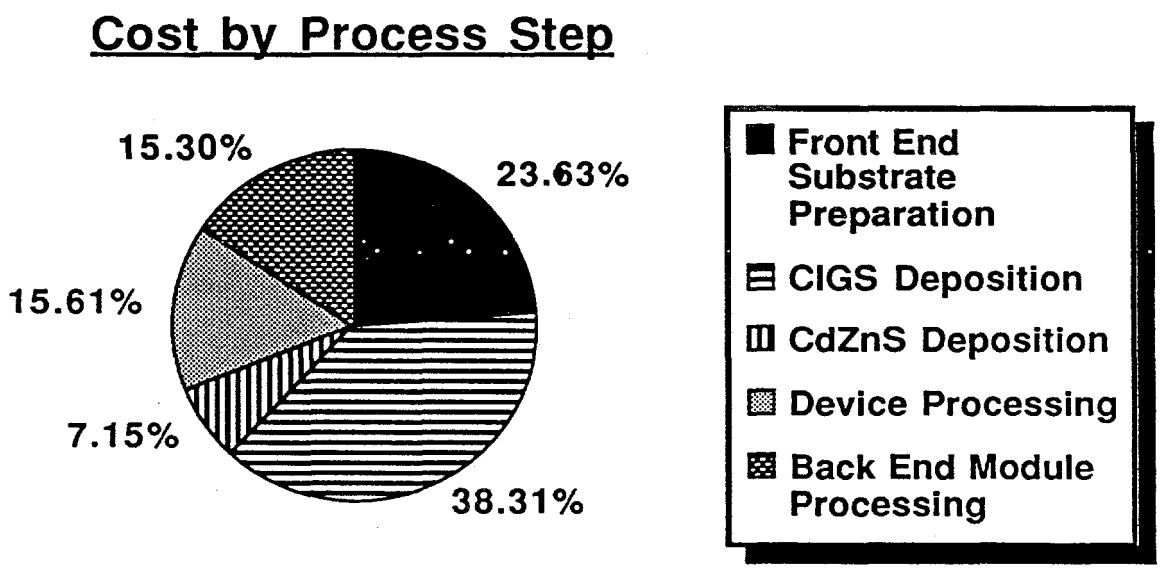

Figure 4.-5: Full-Scale Inline CIGS Module Product Cost Breakdown by Process Step

5. PLAN FOR THE DEVELOPMENT OF THE PROPOSED PROCESSES AND EQUIPMENT

We have developed a preliminary plan to design, build and test the Prototype Inline CIGS Module Production Plant previously described in this report. Our development program scheduling has led us to conclude that this effort can be concluded in *three* years, and at an *estimated* expense of ~$14M. Completely detailed program cost estimation has not been performed, hence it is important to remember that this cost estimate is tentative. A breakdown of the costs leading to this estimate is presented in table 5.-1 below.

Estimated Expenses ($K)	Year 1	Year 2	Year 3	
Facility	$60	$60	$60	
General Office	$75	$80	$90	
Management & Engineering	$850	$850	$850	
Travel	$30	$40	$50	
Capital Equipment	$4,500	$2,500	$1,000	
Labor	$300	$400	$600	
Material	$100	$400	$700	
Energy	$50	$125	$200	TOTAL ($K)
Annual Totals	$5,965	$4,455	$3,550	$13,970

Table 5.-1: Prototype Inline CIGS Manufacturing Technology Development Program Preliminary Cost Estimate

Our determination that this program can be completed in three years is based on our estimates of the time required to complete each task and an analysis of the development activities interrelationships. Figure 5.-2 is a PERT chart which displays these relationships, and the resulting development schedule comprises figure 5.-3.

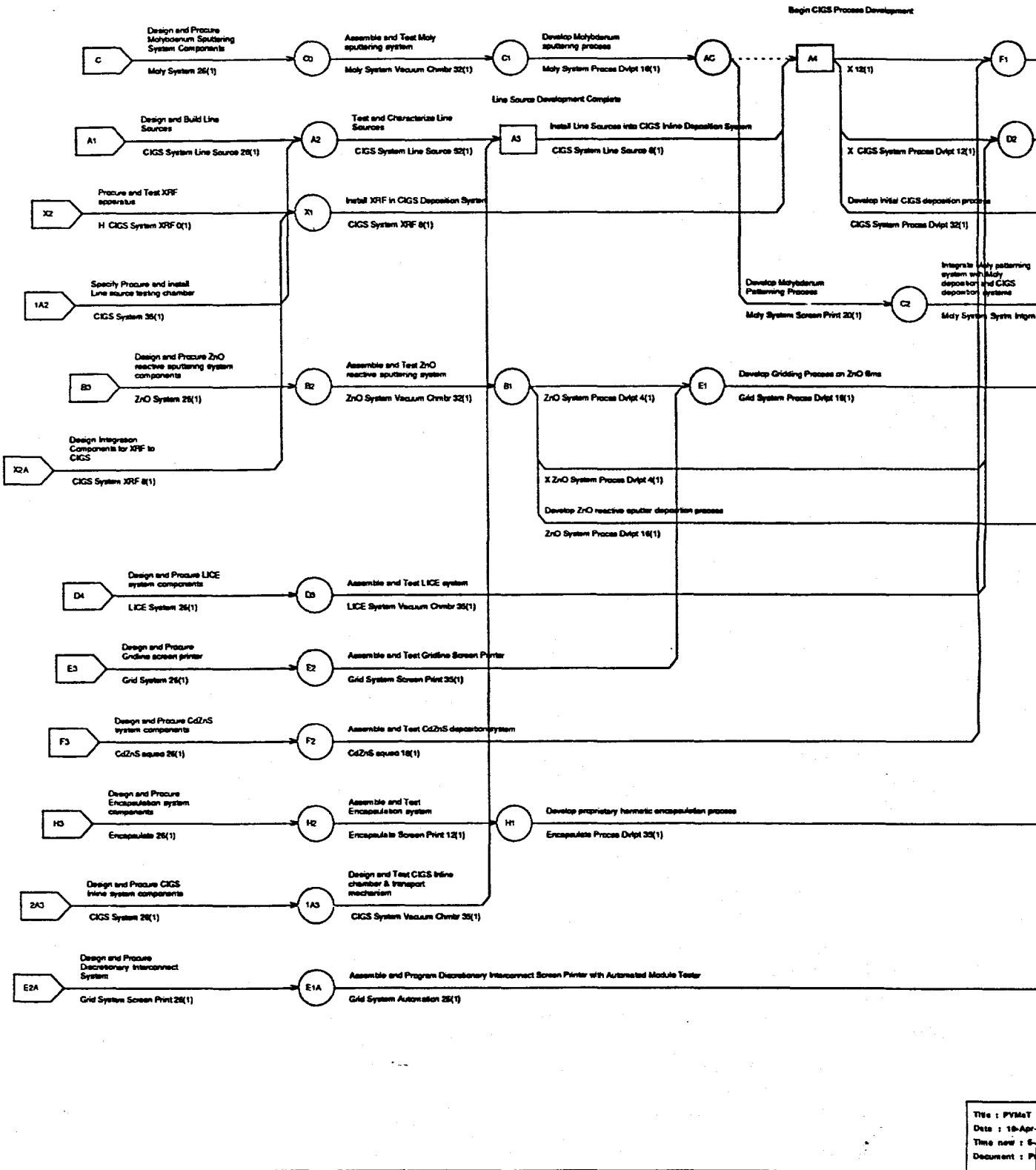

Figure 5.-2: PERT Chart for Prototype Inline CIGS Module Manufacturing Technology Development Program

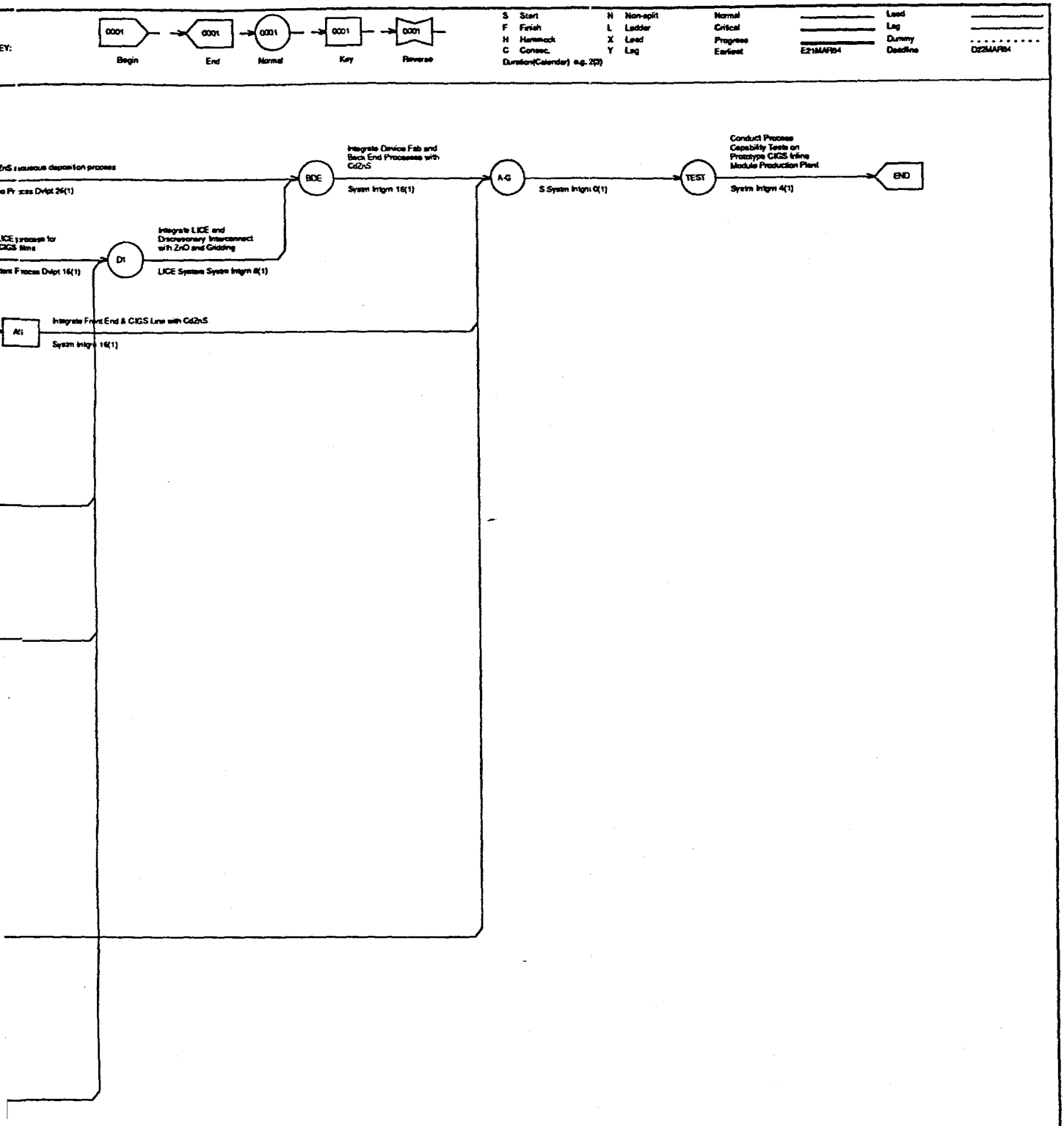
EY:
0001
Begin
0001
End
0001
Normal
0001
Key
0001
Reverse
S Start
F Finish
H Hammock
C Consec.
Duration(Calendar) e.g. 2(3)
N Non-split
L Ladder
X Lead
Y Lag
Normal
Critical
Progress
Earliest
E21MAR84
Lead
Lag
Dummy
Deadline
D23MAR84
ZnS vaueous deposition process
Pr ocess Dvlpt 26(1)
Integrate Device Fab and Back End Processes with Cd2nS
BDE
System Intgrn 16(1)
A-G
S System Intgrn 0(1)
Conduct Process Capability Tests on Prototype CIGS Inline Module Production Plant
TEST
System Intgrn 4(1)
END
ICE) process for CIGS films
tem Frocss Dvlpt 16(1)
Integrate LICE and Discretionary Interconnect with ZnO and Gridding
DI
LICE System System Intgrn 8(1)
AG
Integrate Front End & CIGS Line with Cd2nS
System Intgrn 16(1)

Date : 10-APR-91
Time Now : 6-JAN-92
Project : PVMaT Phase
Output : Time analysis dule
Sheet : 1 of 1

		EARLY Start	EARLY Finish	LATE Start	LATE Finish	Duration	Events Prec	Events Succ
Systm Intgrn	Integrate Front End & CIGS Line with CdZnS	13Jun 94	30Sep 94	25Jul 94	11Nov 94	16,0	A5	A-G
	Integrate Device Fab and Back End Processes with CdZnS	25Jul 94	11Nov 94	25Jul 94	11Nov 94	16,0	BDE	A-G
		14Nov 94		14Nov 94		0,0	A-G	TEST
	Conduct Process Capability Tests on Prototype CIGS Inline Module Production Plant	14Nov 94	9Dec 94	14Nov 94	9Dec 94	4,0	TEST	END
CIGS System	Design and Procure CIGS Inline system components	MIN	3Jul 92	6Jul 92	1Jan 93	26,0	2A3	1A3
	Specify Procure and install Line source testing chamber	MIN	4Sep 92	MIN	4Sep 92	35,0	1A2	A2
Line Source	Design and Build Line Sources	MIN	17Jul 92	24Feb 92	4Sep 92	28,0	A1	A2
	Test and Characterize Line Sources	7Sep 92	3Sep 93	7Sep 92	3Sep 93	52,0	A2	A3
	Install Line Sources into CIGS Inline Deposition System	6Sep 93	29Oct 93	6Sep 93	29Oct 93	8,0	A3	A4
Vacuum Chmbr	Design and Test CIGS Inline chamber & transport mechanism	6Jul 92	5Mar 93	4Jan 93	3Sep 93	35,0	1A3	A3
XRF	Procure and Test XRF apparatus	MIN	28Feb 92	MIN	3Sep 93	8,0	X2	X1
	Design Integration Components for XRF to CIGS	MIN	28Feb 92	12Jul 93	3Sep 93	8,0	X2A	X1
	Install XRF in CIGS Deposition System	2Mar 92	24Apr 92	6Sep 93	29Oct 93	8,0	X1	A4
Process Dvlpt	Develop initial CIGS deposition process	1Nov 93	10Jun 94	13Dec 93	22Jul 94	32,0	A4	A5
ZnO System	Design and Procure ZnO reactive sputtering system components	MIN	3Jul 92	30Nov 92	28May 93	26,0	B3	B2
Vacuum Chmbr	Assemble and Test ZnO reactive sputtering system	6Jul 92	12Feb 93	31May 93	7Jan 94	32,0	B2	B1
Process Dvlpt		15Feb 93	12Mar 93	10Jan 94	4Feb 94	4,0	B1	E1
	Develop ZnO reactive sputter deposition process	15Feb 93	4Jun 93	7Feb 94	27May 94	16,0	B1	D1
Moly System	Design and Procure Molybdenum Sputtering System Components	MIN	3Jul 92	1Jun 92	27Nov 92	26,0	C	C0
Vacuum Chmbr	Assemble and Test Moly sputtering system	6Jul 92	12Feb 93	30Nov 92	9Jul 93	32,0	C0	C1
Screen Print	Develop Molybdenum Patterning Process	7Jun 93	22Oct 93	15Nov 93	1Apr 94	20,0	AC	C2
Systm Intgrn	Integrate Moly patterning system with Moly deposition and CIGS deposition systems	25Oct 93	11Feb 94	4Apr 94	22Jul 94	16,0	C2	A5
Process Dvlpt	Develop Molybdenum sputtering process	15Feb 93	4Jun 93	12Jul 93	29Oct 93	16,0	C1	AC
LICE System	Design and Procure LICE system components	MIN	3Jul 92	7Dec 92	4Jun 93	26,0	D4	D3
Vacuum Chmbr	Assemble and Test LICE system	6Jul 92	5Mar 93	7Jun 93	4Feb 94	35,0	D3	D2
Systm Intgrn	Integrate LICE and Discretionary Interconnect with ZnO and Gridding	16May 94	8Jul 94	30May 94	22Jul 94	8,0	D1	BDE
Process Dvlpt	Develop LICE process for ZnO and CIGS films	24Jan 94	13May 94	7Feb 94	27May 94	16,0	D2	D1
Grid System	Design and Procure Gridline screen printer	MIN	3Jul 92	7Dec 92	4Jun 93	26,0	E3	E2
Screen Print	Design and Procure Discretionary Interconnect System	MIN	3Jul 92	31May 93	26Nov 93	26,0	E2A	E1A
	Assemble and Test Gridline Screen Printer	6Jul 92	5Mar 93	7Jun 93	4Feb 94	35,0	E2	E1
Automation	Assemble and Program Discretionary Interconnect Screen Printer with Automated Module Tester	6Jul 92	1Jan 93	29Nov 93	27May 94	26,0	E1A	D1
Process Dvlpt	Develop Gridding Process on ZnO films	15Mar 93	2Jul 93	7Feb 94	27May 94	16,0	E1	D1
CdZnS aqueo	Design and Procure CdZnS system components	MIN	3Jul 92	22Mar 93	17Sep 93	26,0	F3	F2
	Assemble and Test CdZnS deposition system	6Jul 92	6Nov 92	20Sep 93	21Jan 94	18,0	F2	F1
Process Dvlpt	Develop CdZnS aqueous deposition process	24Jan 94	22Jul 94	24Jan 94	22Jul 94	26,0	F1	BDE
Encapsulate	Design and Procure Encapsulation system components	MIN	3Jul 92	21Jun 93	17Dec 93	26,0	H3	H2
Screen Print	Assemble and Test Encapsulation system	6Jul 92	25Sep 92	20Dec 93	11Mar 94	12,0	H2	H1
Process Dvlpt	Develop proprietary hermetic encapsulation process	28Sep 92	28May 93	14Mar 94	11Nov 94	35,0	H1	A-G

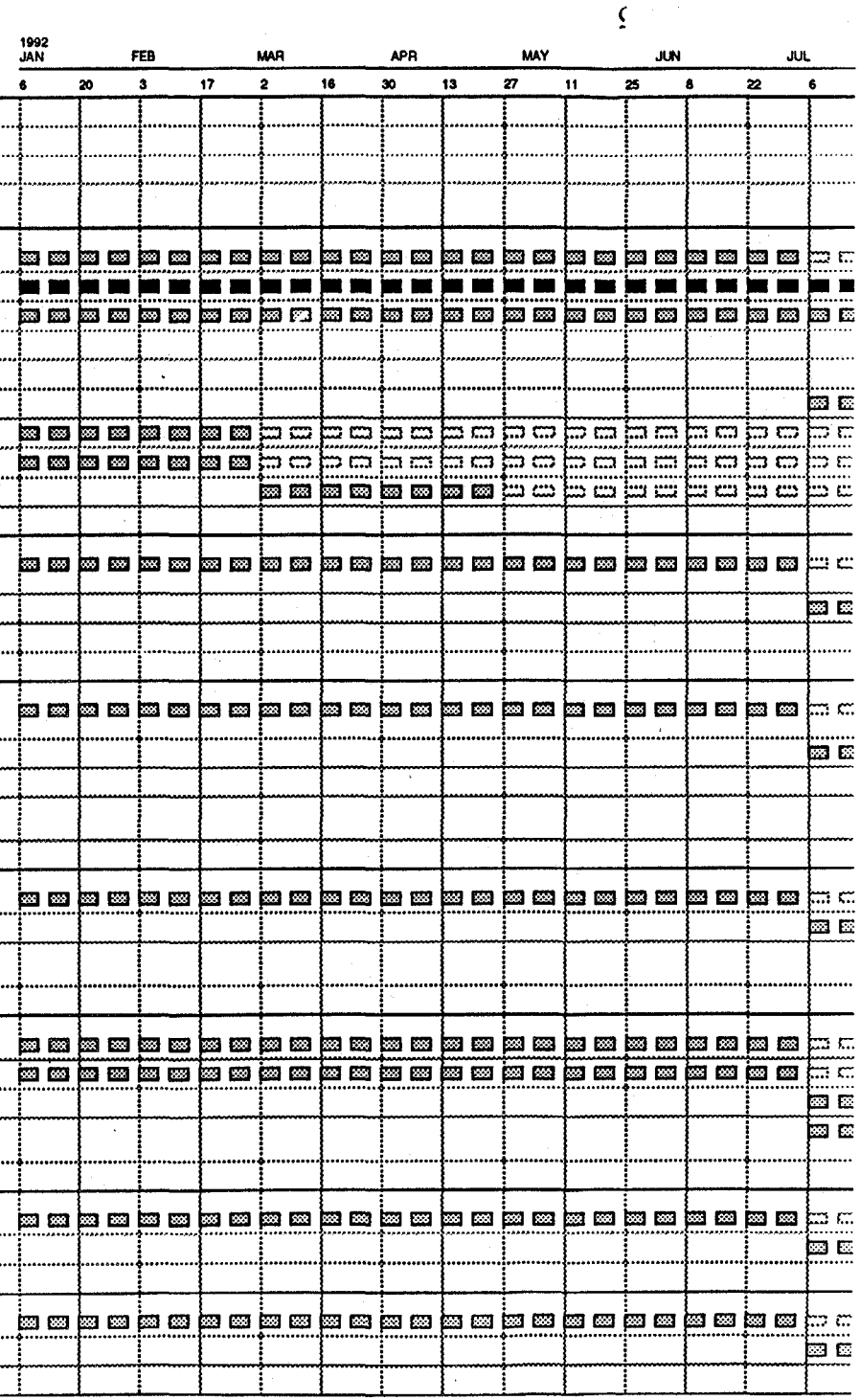

Figure 5.-2: Schedule for Prototype Inline CIGS Module Manufacturing Technology Development Program [Part 1]

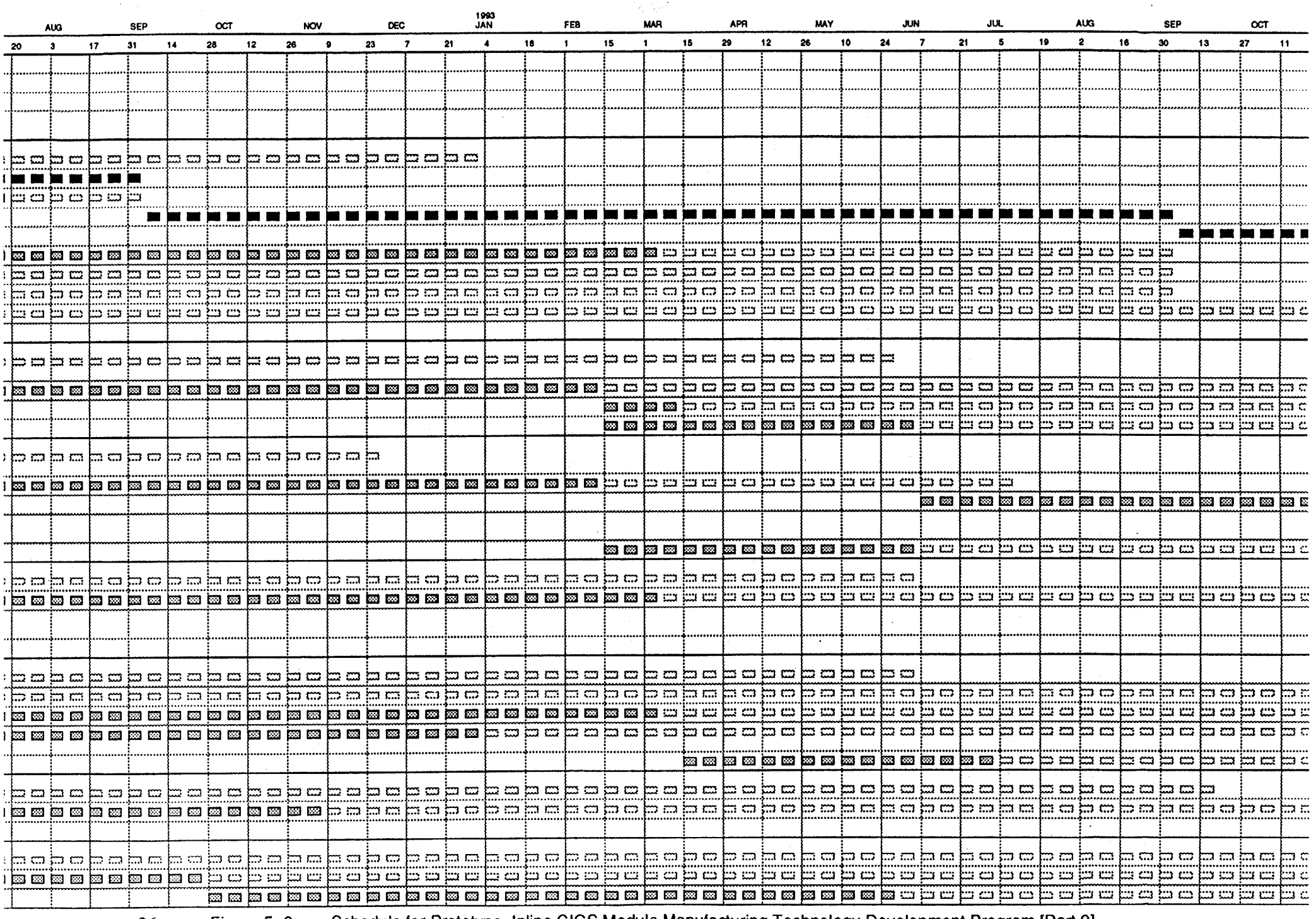

Figure 5.-2: Schedule for Prototype Inline CIGS Module Manufacturing Technology Development Program [Part 2]

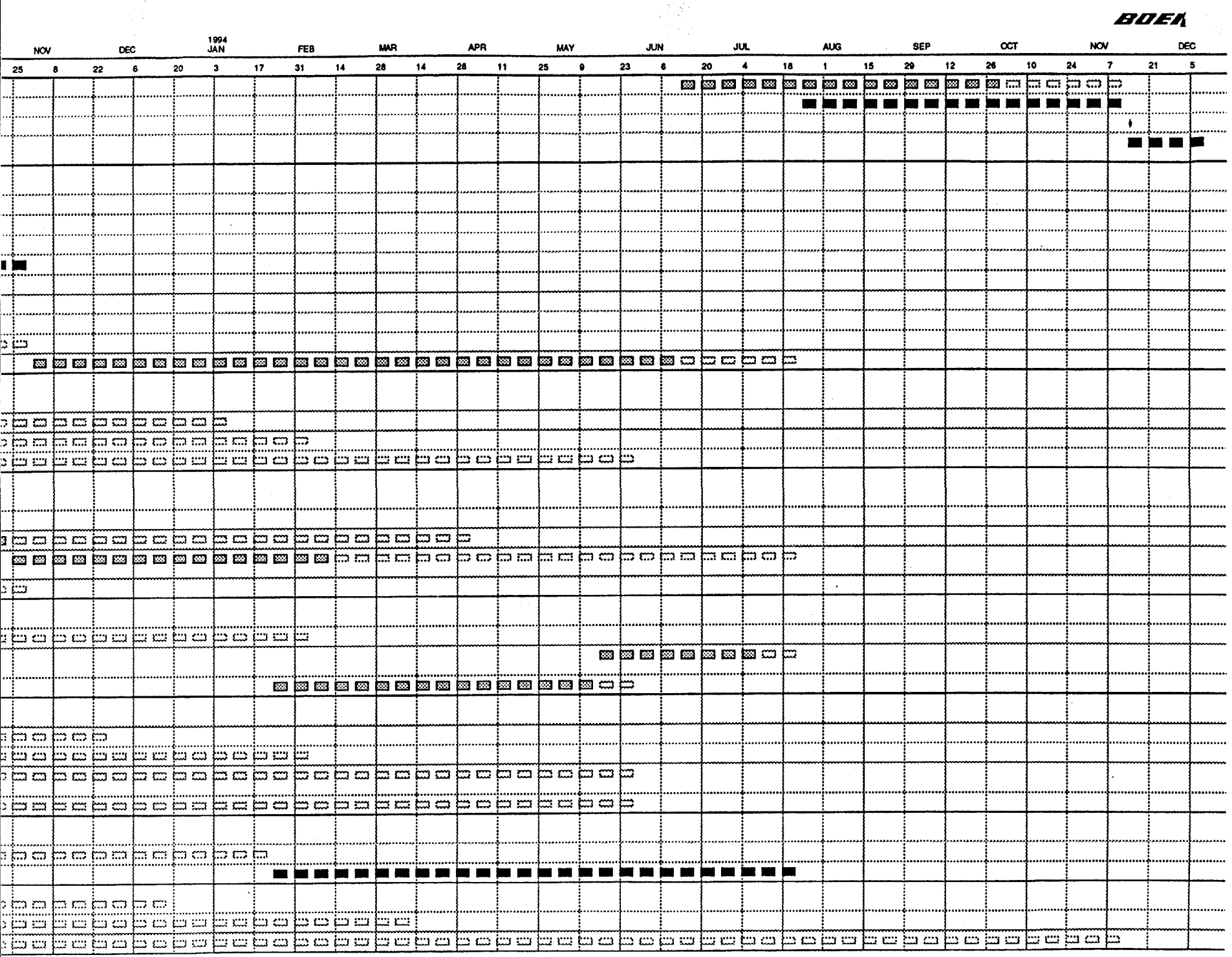

Figure 5.-2: Schedule for Prototype Inline CIGS Module Manufacturing Technology Development Program [Part 3]

6. SUMMARY: CIGS MODULES—SOLVING THE PV COST PROBLEM

The manufacturing technology for achieving the goals of the PVMaT project has three aspects: the product, the process, and the equipment. We anticipate that the implementation of advanced semiconductor device fabrication techniques to the production of large–area $CuIn_{1-x}Ga_xSe_2$ /$Cd_{1-y}Zn_yS$/ZnO monolithically integrated thin–film solar cell modules will enable 15% median efficiencies to be achieved in high volume manufacturing. We do not believe that CIS can achieve this efficiency in production without sufficient gallium to significantly increase the bandgap, thereby matching it better to the solar spectrum (i.e., $x \geq 0.2$). Competing techniques for $CuInSe_2$ film formation have not been successfully extended to CIGS devices with such high bandgaps. The long-term stability of CIGS module performance is expected to depend entirely on the quality of their hermetic encapsulation and the stability of any polymeric lamination materials under extended exposure to UV radiation. The SERI–confirmed intrinsic stability of CIS–based photovoltaics renders them far superior to α-Si:H-based devices, making a 30-year module lifetime feasible. The minimal amounts of cadmium used in the structure we propose compared to CdTe-based devices makes them environmentally safer and more acceptable to both consumers and relevant regulatory agencies. This will significantly reduce the cost of production facilities for thin–film cells by minimizing waste disposal, hazardous material handling, environmental protection, and occupational safety related capital and operating expenses. The simplicity and reliability of the balance–of–systems (BOS) requirements for fixed flat plate solar arrays ensure this technology a majority share of the market when compared to concentrator solar arrays. In addition, flat plate thin–film technology can utilize all the available light, not just the direct component, and operate under conditions of partial solar obscuration that render concentrators useless. Large–area integrated thin–film CIGS modules are the product most likely to supplant silicon modules by the end of this decade and enable the cost improvements which will lead to rapid market expansion.

The cost analysis of the small scale batch fabrication process for CIS submodules currently implemented in the Boeing PSDL presented in §2.4 identified the key themes of our solution: ***automation; continuous inline processing; high throughput; large–area substrates.*** The analysis of module power costs presented in §4 and Appendix A substantiate our contention that the goals of the PVMaT Initiative can be achieved by taking the next step to develop the manufacturing technology infrastructure for large–area inline CIGS module production systems. It is not PV modules themselves, but the manufacturing equipment which enables their low–cost production in which the United States must establish and maintain a technological advantage over other nations if we are to become and remain the primary economic benefactors of the inevitable growth of the photovoltaics industry in the 21st century.

	Process Description	'97 Scenario Yield	'97 Scenario CumVal_1x4	First Generation Production Capability '94 Scenario		'95 Scenario		'96 Scenario	
Step1	Front End Substrate Preparation	0.99	$11.70	0.96	$11.96	0.97	$11.83	0.98	$11.73
Step2	CIGS Deposition	0.97	$35.84	0.92	$38.18	0.94	$37.07	0.96	$36.09
Step3	CdZnS Deposition	0.98	$41.05	0.90	$47.36	0.92	$45.09	0.98	$41.30
Step4	Device Processing	0.99	$50.32	0.94	$60.42	0.96	$56.53	0.95	$52.70
Step5	Back End Module Processing	0.97	$71.49	0.88	$91.65	0.90	$84.75	0.93	$77.38
	Net CIGS Yield	**90%**		**66%**		**72%**		**81%**	
	Unscheduled Downtime	6%		20%		15%		10%	
	Total Uptime	**80%**		**66%**		**71%**		**76%**	

SubModule width:	12	inches	
SubModule length:	48	inches	
Number of Submodules per Module:	6	each	
Module Area:	2.23	m^2	
Output Capacity (CIGS submodules/year):	74,635		47,342	55,445	65,744
Rated Module Power @ AM1.5G Efficiency of **15.0%**	**324**	Watts	**12.0%** **260**	**13.0%** **281**	**14.0%** **303**
Annual Module Production	12,439	/yr	**7,890**	**9,241**	**10,957**
Annual Power Production	4.04	MW/yr	**2.05**	**2.60**	**3.32**
Module Cost	$428.94	$/Module	**$549.92**	**$508.50**	**$464.27**
Initial Peak Power Cost	$1.32	$/W	**$2.12**	**$1.81**	**$1.53**
Peak Power Cost after full capital depreciation	$0.75	$/W	**$1.16**	**$1.01**	**$0.87**
Areal Module Cost (Initial)	$192.38	$/m^2	**$246.64**	**$228.06**	**$208.22**
Areal Module Cost (Recurring)	$109.22	$/m^2	**$135.06**	**$126.83**	**$117.83**

Item	Lot Cost	Lot Qty	Units	Cost	Units
Molybdenum target	$10,534	0.5	inches thick	$10,534.0000	ea
Copper	$10	5	lb	$0.0044	$/gm
Indium	$875	2.5	kg	$0.3500	$/gm
Gallium	$1,330	2.5	kg	$0.5320	$/gm
Selenium	$44	2.5	kg	$0.0176	$/gm
Cadmium Chloride	$380	3	kg	$0.1267	$/gm
Zinc Chloride	$671	12	kg	$0.0559	$/gm
Ammonium Chloride	$170	10	kg	$0.0170	$/gm
Thiourea	$525	12	kg	$0.0438	$/gm
Ammonium Hydroxide [15M]	$95	15	liters	$6.3333	liter
glass substrates 4' x 13" x 3/16"	$0.60	1	sq ft	$2.60	ea
Metalization screen-print Ink	$1,100	1	kg	$1.1000	$/gm
Zinc (+2% Aluminum) target	$3,045	0.5	inches thick	$3,045.0000	ea
Argon	$2.92	500	liters	$0.0058	liter
Oxygen	$7.64	500	liters	$0.0153	liter
LICE Etch Gas	$297	100	lb	$0.0065	$/gm
Electricity				$0.0450	$/kWh
Operators:Fully Fringe-Burdened Wage	$4,320	1	week	$30.00	$/operator-hr
Laser Operating Expense				$10.4350	$/operating-hr
Moly Etch Reagant 1	$70	3	kg	$0.0233	$/gm
Moly Etch Reagant 2	$95	10	kg	$0.0095	$/gm
Moly Etch Maskant				$0.0300	liter
Module Sealant	$22	1	lb	$0.0488	$/gm
Low-iron glass superstrates 4'x6'x1/4"	$0.70	1	sq ft	$16.80	ea
---	---	---	---	---	---
Number of Shifts	3	scheduled			
Work-hours/week	144	weekly uptime=	86%		
Work-weeks/year	50	% of weekly scheduled			
labor efficiency factor (0≤eff≤1)	75%	uptime realized=	94%		

Item	Annual Utilization (lots)	Annual Expense	% of Subtotal	Layer	% of Materials Expense
Molybdenum target	4	$35,898	2%	Glass	29%
Copper	120	$1,202	0%	Moly	2%
Indium	166	$145,147	10%	CIGS	15%
Gallium	36	$48,161	3%	CdZnS	8%
Selenium	682	$30,030	2%	ZnO	2%
Cadmium Chloride	129	$49,182	3%	Grid & Buss	41%
Zinc Chloride	5	$3,233	0%	consumables	4%
Ammonium Chloride	38	$6,497	0%		
Thiourea	107	$56,092	4%		
Ammonium Hydroxide [15M]	17	$1,601	0%		
glass substrates 4' x 13" x 3/16"	82,585	$214,721	14%		
Metalization screen-print Ink	569	$625,639	41%		
Zinc (+2% Aluminum) target	4	$9,623	1%		
Argon	2,031	$5,948	0%		
Oxygen	1,993	$15,227	1%		
LICE Etch Gas	32	$9,383	1%		
Electricity	7,807,978	$351,359			
Operators:Fully Fringe-Burdened Wage	5.17	$1,161,861			
Laser Operating Expense		$35,312	2%		
Moly Etch Reagant 1	33,279	$2,330	0%		
Moly Etch Reagant 2	2,170	$506	0%		
Moly Etch Maskant	430	$13	0%		
Module Sealant	2	$4,763	0%		
Low-iron glass superstrates 4'x6'x1/4"	12,824	$215,440	14%		
---		---			
	Total Annual Materials $:	**$1,515,949**			
	Total Annual Labor $:	**$1,161,861**			
	Total Annual Energy $:	**$351,359**			

'94 Scenario			Reverse						
	Cost by Process Step		Cum Yield	Materials	Energy	Labor	Depreciation	$/Step	Cum$/Step
Step1	Front End Substrate Preparation	**19%**	0.66	$4.79	$1.89	$3.80	$6.98	$17.46	$17.46
Step2	CIGS Deposition	**37%**	0.68	$4.01	$1.76	$6.94	$21.11	$33.82	$51.28
Step3	CdZnS Deposition	**7%**	0.74	$1.97	$0.06	$2.83	$1.10	$5.97	$57.25
Step4	Device Processing	**12%**	0.83	$1.06	$1.18	$3.30	$5.86	$11.40	$68.66
Step5	Back End Module Processing	**25%**	0.88	$12.50	$1.27	$2.82	$6.42	$23.00	$91.65
				Materials	**Energy**	**Labor**	**Depreciation**		convergence:
	Cost by Category			**27%**	**7%**	**21%**	**45%**		0.00

				total vs. by-part	
Production Volume (MW/yr):	2.05			convergence by category:	
Annual Production (#modules):	7,890				
Total Annual Direct Materials Expense:	$1,151,917	$145.99	[per module]	$0	$1,151,917
Total Annual Direct Energy Expense:	$291,867	$36.99	[per module]	$0	$291,867
Total Annual Direct Labor ($labor/yr)	$932,271	4.15	[staff/shift]	$0	$932,271
Total Annual Direct Depreciation Expense	$1,963,000	5.00	[SLD period (yrs)]	$0	$1,963,000
Factory Labor:	**12.45**	persons, each @ 40 hrs/wk			
Total Equipment Capital Expense	**$12,941,250**				

'95 Scenario			Reverse						
	Cost by Process Step		Cum Yield	Materials	Energy	Labor	Depreciation	$/Step	Cum$/Step
Step1	Front End Substrate Preparation	**19%**	0.72	$4.35	$1.72	$3.44	$6.33	$15.84	$15.84
Step2	CIGS Deposition	**36%**	0.75	$3.68	$1.61	$6.36	$19.16	$30.80	$46.64
Step3	CdZnS Deposition	**7%**	0.79	$1.85	$0.06	$2.65	$1.00	$5.55	$52.19
Step4	Device Processing	**13%**	0.86	$1.02	$1.13	$3.16	$5.31	$10.62	$62.81
Step5	Back End Module Processing	**26%**	0.90	$12.22	$1.16	$2.74	$5.82	$21.94	$84.75
				Materials	**Energy**	**Labor**	**Depreciation**		convergence:
	Cost by Category			**27%**	**7%**	**22%**	**44%**		0.00

Production Volume (MW/yr):	2.60			total vs. by-part	
Annual Production (#modules):	9,241			convergence by category:	
Total Annual Direct Materials Expense:	$1,281,452	$138.67	[per module]	$0	$1,281,452
Total Annual Direct Energy Expense:	$314,164	$34.00	[per module]	$0	$314,164
Total Annual Direct Labor ($labor/yr)	$1,017,635	4.53	[staff/shift]	$0	$1,017,635
Total Annual Direct Depreciation Expense	$2,085,688	5.00	[SLD period (yrs)]	$0	$2,085,688
Factory Labor:	**13.59**	persons, each @ 40 hrs/wk			
Total Equipment Capital Expense	**$12,941,250**				

'96 Scenario			Reverse						
	Cost by Process Step		Cum Yield	Materials	Energy	Labor	Depreciation	$/Step	Cum$/Step
Step1	Front End Substrate Preparation	**18%**	0.81	$3.86	$1.53	$3.06	$5.65	$14.11	$14.11
Step2	CIGS Deposition	**36%**	0.83	$3.30	$1.44	$5.72	$17.11	$27.57	$41.68
Step3	CdZnS Deposition	**7%**	0.87	$1.70	$0.05	$2.43	$0.89	$5.07	$46.75
Step4	Device Processing	**13%**	0.88	$1.01	$1.09	$3.08	$4.74	$9.92	$56.67
Step5	Back End Module Processing	**27%**	0.93	$11.82	$1.04	$2.65	$5.20	$20.71	$77.38
				Materials	**Energy**	**Labor**	**Depreciation**		convergence:
	Cost by Category			**28%**	**7%**	**22%**	**43%**		0.00

				total vs. by-part	
Production Volume (MW/yr):	3.32				
Annual Production (#modules):	10,957			convergence by category:	
Total Annual Direct Materials Expense:	$1,426,862	$130.22	[per module]	$0	$1,426,862
Total Annual Direct Energy Expense:	$338,862	$30.93	[per module]	$0	$338,862
Total Annual Direct Labor ($labor/yr)	$1,113,073	4.95	[staff/shift]	$0	$1,113,073
Total Annual Direct Depreciation Expense	$2,208,375	5.00	[SLD period (yrs)]	$0	$2,208,375
Factory Labor:	**14.86**	persons, each @ 40 hrs/wk			
Total Equipment Capital Expense	**$12,941,250**				

'97 Scenario			Reverse						
	Cost by Process Step		Cum Yield	Materials	Energy	Labor	Depreciation	$/Step	Cum$/Step
Step1	Front End Substrate Preparation	**18%**	0.90	$3.47	$1.38	$2.76	$5.20	$12.82	$12.82
Step2	CIGS Deposition	**35%**	0.91	$3.01	$1.32	$5.21	$15.74	$25.27	$38.09
Step3	CdZnS Deposition	**7%**	0.94	$1.56	$0.05	$2.23	$0.82	$4.66	$42.75
Step4	Device Processing	**13%**	0.96	$0.93	$1.00	$2.83	$4.36	$9.13	$51.88
Step5	Back End Module Processing	**27%**	0.97	$11.34	$0.96	$2.53	$4.78	$19.61	$71.49
				Materials	**Energy**	**Labor**	**Depreciation**		convergence:
	Cost by Category			**28%**	**7%**	**22%**	**43%**		0.00

				total vs. by-part	
Production Volume (MW/yr):	4.04			convergence by category:	
Annual Production (#modules):	12,439				
Total Annual Direct Materials Expense:	$1,515,933	$121.87	[per module]	$0	$1,515,933
Total Annual Direct Energy Expense:	$351,359	$28.25	[per module]	$0	$351,359
Total Annual Direct Labor ($labor/yr)	$1,161,861	5.17	[staff/shift]	$0	$1,161,861
Total Annual Direct Depreciation Expense	$2,306,525	5.00	[SLD period (yrs)]	$0	$2,306,525
Factory Labor:	**15.52**	persons, each @ 40 hrs/wk			
Total Equipment Capital Expense	**$12,941,250**				

	Process Description	2000 Scenario Yield	2000 Scenario CumVal_1x4	Second Generation Production Capability '97 Scenario		'98 Scenario		'99 Scenario	
Step1	Front End Substrate Preparation	0.99	$39.68	0.96	$40.43	0.97	$40.01	0.98	$39.82
Step2	CIGS Deposition	0.97	$107.23	0.92	$113.56	0.94	$110.24	0.96	$108.04
Step3	CdZnS Deposition	0.98	$122.04	0.90	$140.03	0.92	$133.30	0.98	$122.87
Step4	Device Processing	0.99	$151.12	0.94	$180.61	0.96	$168.87	0.95	$158.35
Step5	Back End Module Processing	0.97	$183.94	0.88	$237.76	0.90	$218.80	0.93	$199.93
	Net CIGS Yield	**90%**		**66%**		**72%**		**81%**	
	Unscheduled Downtime	6%		20%		15%		10%	
	Total Uptime	**80%**		**66%**		**71%**		**76%**	
	SubModule width:	48	inches						
	SubModule length:	72	inches						
	Number of Submodules per Module:	1	each						
	Module Area:	2.23	m^2						
	Output Capacity (CIGS submodules/year):	51,971			33,418		39,138		45,780
	Rated Module Power @ AM1.5G Efficiency of **15.0%**	**324**	Watts	**12.0%**	**260**	**13.0%**	**281**	**14.0%**	**303**
	Annual Module Production	**51,971**	/yr		**33,418**		**39,138**		**45,780**
	Annual Power Production	**16.86**	MW/yr		**8.67**		**11.00**		**13.86**
	Module Cost	**$183.94**	$/Module		**$237.76**		**$218.80**		**$199.93**
	Initial Peak Power Cost	**$0.57**	$/W		**$0.92**		**$0.78**		**$0.66**
	Peak Power Cost after full capital depreciation	**$0.31**	$/W		**$0.49**		**$0.42**		**$0.36**
	Areal Module Cost (Initial)	**$82.50**	$/m^2		**$106.64**		**$98.13**		**$89.67**
	Areal Module Cost (Recurring)	**$44.72**	$/m^2		**$56.64**		**$52.77**		**$48.61**

Item	Lot Cost	Lot Qty	Units	Cost	Units
Molybdenum target	$10,534	0.5	inches thick	$10,534.0000	ea
Copper	$10	5	lb	$0.0044	$/gm
Indium	$875	2.5	kg	$0.3500	$/gm
Gallium	$1,000	2.5	kg	$0.4000	$/gm
Selenium	$44	2.5	kg	$0.0176	$/gm
Cadmium Chloride	$380	3	kg	$0.1267	$/gm
Zinc Chloride	$671	12	kg	$0.0559	$/gm
Ammonium Chloride	$170	10	kg	$0.0170	$/gm
Thiourea	$525	12	kg	$0.0438	$/gm
Ammonium Hydroxide [15M]	$95	15	liters	$6.3333	liter
glass substrates 6.2' x 4' x 1/2"	$0.78	1	sq ft	$19.50	ea
Metalization screen-print Ink	$1,100	1	kg	$1.1000	$/gm
Zinc (+2% Aluminum) target	$3,570	0.5	inches thick	$3,570.0000	ea
Argon	$2.92	500	liters	$0.0058	liter
Oxygen	$7.64	500	liters	$0.0153	liter
LICE Etch Gas	$297	100	lb	$0.0065	$/gm
Electricity				$0.0450	$/kWh
Operators:Fully Fringe-Burdened Wage	$4,320	1	week	$30.00	$/operator-hr
Laser Operating Expense				$10.4350	$/operating-hr
Moly Etch Reagant 1	$70	3	kg	$0.0233	$/gm
Moly Etch Reagant 2	$95	10	kg	$0.0095	$/gm
Moly Etch Maskant				$0.0300	liter
Module Sealant	$22	1	lb	$0.0488	$/gm
Low-iron glass superstrates 4'x6'x1/4"	$0.80	1	sq ft	$19.20	ea
---	---	---	---	---	---
Number of Shifts	3	scheduled			
Work-hours/week	144	weekly uptime=	86%		
Work-weeks/year	50	% of weekly scheduled			
labor efficiency factor (0≤eff≤1)	75%	uptime realized=	94%		

Item	Annual Utilization (lots)	Annual Expense	% of Subtotal	Layer	% of Materials Expense	
Molybdenum target	4	$39,437	1%	Glass	56%	
Copper	457	$4,572	0%	Moly	1%	
Indium	631	$552,194	14%	CIGS	21%	
Gallium	138	$137,762	4%	CdZnS	12%	
Selenium	2,596	$114,245	3%	ZnO	2%	
Cadmium Chloride	499	$189,679	5%	consumables	8%	
Zinc Chloride	19	$12,469	0%			
Ammonium Chloride	147	$25,058	1%			
Thiourea	412	$216,328	6%			
Ammonium Hydroxide [15M]	65	$6,174	0%			
glass substrates 6.2' x 4' x 1/2"	57,507	$1,121,390	29%			
Metalization screen-print Ink	0	$0	0%			
Zinc (+2% Aluminum) target	4	$12,602	0%			
Argon	1,979	$5,790	0%			
Oxygen	7,972	$60,909	2%			
LICE Etch Gas	47	$14,074	0%			
Electricity	7,916,485	$356,242				
Operators:Fully Fringe-Burdened Wage	4.38	$984,317				
Laser Operating Expense		$282,496	7%			
Moly Etch Reagant 1	129,541	$9,068	0%			
Moly Etch Reagant 2	8,449	$1,971	0%			
Moly Etch Maskant	1,795	$54	0%			
Module Sealant	3	$6,634	0%			
Low-iron glass superstrates 4'x6'x1/4"	53,578	$1,028,706	27%			
	Total Annual Materials $:	**$3,841,614**				
	Total Annual Labor $:	**$984,317**				
	Total Annual Energy $:	**$356,242**				

'97 Scenario			Reverse						
	Cost by Process Step		Cum Yield	Materials	Energy	Labor	Depreciation	$/Step	Cum$/Step
Step1	Front End Substrate Preparation	**25%**	0.66	$31.19	$2.68	$5.38	$19.77	$59.03	$59.03
Step2	CIGS Deposition	**39%**	0.68	$20.74	$3.44	$9.50	$59.82	$93.50	$152.53
Step3	CdZnS Deposition	**7%**	0.74	$10.94	$0.36	$2.89	$2.56	$16.76	$169.29
Step4	Device Processing	**15%**	0.83	$8.23	$1.86	$4.74	$21.11	$35.95	$205.24
Step5	Back End Module Processing	**14%**	0.88	$21.96	$0.61	$1.74	$8.21	$32.53	$237.76
				Materials	**Energy**	**Labor**	**Depreciation**		convergence:
	Cost by Category			**39%**	**4%**	**10%**	**47%**		0.00

Production Volume (MW/yr):	8.67			total vs. by-part	
Annual Production (#modules):	33,418			convergence by category:	
Total Annual Direct Materials Expense:	$3,110,070	$93.07	[per module]	$0	$3,110,070
Total Annual Direct Energy Expense:	$299,379	$8.96	[per module]	$0	$299,379
Total Annual Direct Labor ($labor/yr)	$810,461	3.61	[staff/shift]	$0	$810,461
Total Annual Direct Depreciation Expense	$3,725,600	5.00	[SLD period (yrs)]	$0	$3,725,600
Factory Labor:	**10.82**	persons, each @ 40 hrs/wk			
Total Equipment Capital Expense	**$24,745,000**				

'98 Scenario			Reverse						
	Cost by Process Step		Cum Yield	Materials	Energy	Labor	Depreciation	$/Step	Cum$/Step
Step1	Front End Substrate Preparation	**24%**	0.72	$28.30	$2.43	$4.88	$17.94	$53.55	$53.55
Step2	CIGS Deposition	**39%**	0.75	$19.01	$3.14	$8.70	$54.27	$85.13	$138.68
Step3	CdZnS Deposition	**7%**	0.79	$10.24	$0.33	$2.70	$2.32	$15.60	$154.29
Step4	Device Processing	**15%**	0.86	$7.89	$1.77	$4.53	$19.16	$33.35	$187.63
Step5	Back End Module Processing	**14%**	0.90	$21.47	$0.56	$1.69	$7.45	$31.17	$218.80
				Materials	**Energy**	**Labor**	**Depreciation**		convergence:
	Cost by Category			**40%**	**4%**	**10%**	**46%**		0.00

				total vs. by-part	
Production Volume (MW/yr):	11.00			convergence by category:	
Annual Production (#modules):	39,138				
Total Annual Direct Materials Expense:	$3,402,032	$86.92	[per module]	$0	$3,402,032
Total Annual Direct Energy Expense:	$322,194	$8.23	[per module]	$0	$322,194
Total Annual Direct Labor ($labor/yr)	$880,710	3.92	[staff/shift]	$0	$880,710
Total Annual Direct Depreciation Expense	$3,958,450	5.00	[SLD period (yrs)]	$0	$3,958,450
Factory Labor:	**11.76**	persons, each @ 40 hrs/wk			
Total Equipment Capital Expense	**$24,745,000**				

'99 Scenario			Reverse						
	Cost by Process Step		Cum Yield	Materials	Energy	Labor	Depreciation	$/Step	Cum$/Step
Step1	Front End Substrate Preparation	**24%**	0.81	$25.16	$2.17	$4.34	$16.24	$47.91	$47.91
Step2	CIGS Deposition	**38%**	0.83	$17.09	$2.83	$7.83	$49.13	$76.88	$124.79
Step3	CdZnS Deposition	**7%**	0.87	$9.41	$0.30	$2.48	$2.10	$14.29	$139.07
Step4	Device Processing	**16%**	0.88	$7.74	$1.70	$4.42	$17.34	$31.20	$170.27
Step5	Back End Module Processing	**15%**	0.93	$20.78	$0.51	$1.62	$6.74	$29.66	$199.93
				Materials	**Energy**	**Labor**	**Depreciation**		convergence:
	Cost by Category			**40%**	**4%**	**10%**	**46%**		0.00

Production Volume (MW/yr):	13.86		total vs. by-part		
Annual Production (#modules):	45,780		convergence by category:		
Total Annual Direct Materials Expense:	$3,670,528	$80.18	[per module]	$0	$3,670,528
Total Annual Direct Energy Expense:	$343,876	$7.51	[per module]	$0	$343,876
Total Annual Direct Labor ($labor/yr)	$947,046	4.22	[staff/shift]	$0	$947,046
Total Annual Direct Depreciation Expense	$4,191,300	5.00	[SLD period (yrs)]	$0	$4,191,300
Factory Labor:	**12.65**	persons, each @ 40 hrs/wk			
Total Equipment Capital Expense	**$24,745,000**				

2000 Scenario			Reverse						
		Cost by Process Step	Cum Yield	Materials	Energy	Labor	Depreciation	$/Step	Cum$/Step
Step1	Front End Substrate Preparation	24%	0.90	$22.66	$1.96	$3.92	$14.94	$43.47	$43.47
Step2	CIGS Deposition	38%	0.91	$15.56	$2.59	$7.13	$45.20	$70.48	$113.95
Step3	CdZnS Deposition	7%	0.94	$8.65	$0.27	$2.28	$1.94	$13.14	$127.09
Step4	Device Processing	16%	0.96	$7.12	$1.57	$4.06	$15.95	$28.70	$155.79
Step5	Back End Module Processing	15%	0.97	$19.92	$0.47	$1.55	$6.20	$28.15	$183.94
				Materials	Energy	Labor	Depreciation		convergence:
		Cost by Category		40%	4%	10%	46%		0.00

Production Volume (MW/yr):	16.86			total vs. by-part	
Annual Production (#modules):	51,971			convergence by category:	
Total Annual Direct Materials Expense:	$3,841,602	$73.92	[per module]	$0	$3,841,602
Total Annual Direct Energy Expense:	$356,242	$6.85	[per module]	$0	$356,242
Total Annual Direct Labor ($labor/yr)	$984,317	4.38	[staff/shift]	$0	$984,317
Total Annual Direct Depreciation Expense	$4,377,580	5.00	[SLD period (yrs)]	$0	$4,377,580
Factory Labor:	**13.15**	persons, each @ 40 hrs/wk			
Total Equipment Capital Expense	**$24,745,000**				

Document Control Page	1. SERI Report No. NREL/TP-214-4606	2. NTIS Accession No. DE92001176	3. Recipient's Accession No.

4. Title and Subtitle

Manufacturing Technology Development for $CuInGaSe_2$ Solar Cell Modules

5. Publication Date
November 1991

6.

7. Author(s)

B.J. Stanbery

8. Performing Organization Rept. No.

9. Performing Organization Name and Address

Boeing Aerospace & Electronics
P.O. Box 3999
Seattle, WA 98124-2499

10. Project/Task/Work Unit No.
PV150101

11. Contract (C) or Grant (G) No.

(C) XC-1-10057-14

(G)

12. Sponsoring Organization Name and Address
National Renewable Energy Laboratory
1617 Cole Blvd.
Golden, CO 80401-3393

13. Type of Report & Period Covered
Subcontract Report
9 January 1991 - 14 April 1991

14.

15. Supplementary Notes
NREL technical monitor: R. Mitchell, (303) 231-1379

16. Abstract (Limit: 200 words)

The report describes research performed by Boeing Aerospace and Electronics under the Photovoltaic Manufacturing Technology project. We anticipate that implementing advanced semiconductor device fabrication techniques to the production of large-area $CuIn_{1-x}Ga_xSe_2$ (CIGS)/$Cd_{1-y}Zn_yS$/ZnO monolithically integrated thin-film solar cell modules will enable 15% median efficiencies to be achieved in high-volume manufacturing. We do not believe that $CuInSe_2$ (CIS) can achieve this efficiency in production without sufficient gallium to significantly increase the band gap, thereby matching it better to the solar spectrum (i.e., $x \geq 0.2$). Competing techniques for CIS film formation have not been successfully extended to CIGS devices with such high band gaps. The SERI-confirmed intrinsic stability of CIS-based photovoltaics renders them far superior to a-Si:H-based devices, making a 30-year module lifetime feasible. The minimal amounts of cadmium used in the structure we propose, compared to CdTe-based devices, makes them environmentally safer and more acceptable to both consumers and relevant regulatory agencies. Large-area integrated thin-film CIGS modules are the product most likely to supplant silicon modules by the end of this decade and enable the cost improvements which will lead to rapid market expansion.

17. Document Analysis

a. Descriptors
photovoltaics ; solar cells ; manufacturing ; thin films ; modules

b. Identifiers/Open-Ended Terms

c. UC Categories
273

18. Availability Statement
National Technical Information Service
U.S. Department of Commerce
5285 Port Royal Road
Springfield, VA 22161

19. No. of Pages
57

20. Price
A04

Form No. 0069E (6-30-87)